The Study of Thermal Expansion and Magnetostriction of Co Substituted NiZn and MnZn Ferrites

by

Md. Mustafizur Rahman

A DISSERTATION SUBMITTED TO THE DEPARTMENT OF PHYSICS, BUET, DHAKA IN PARTIAL FULFILMENT OF THE REQUIREMENT FOR THE DEGREE OF MASTER OF PHILOSOPHY

BANGLADESH UNIVERSITY OF ENGINEERING AND TECHNOLOGY, DHAKA - 1000, BANGLADESH
2003

The thesis titled, "The Study of Thermal Expansion and Magnetostriction of Co substituted NiZn and MnZn Ferrites" Submitted by Md. Mustafizur Rahaman, Roll No: 9514012F, Session 1994 –95-96, has been accepted as satisfactory in partial fulfillment for the degree of Master of Philosophy in Physics on 26th January, 2003.

BOARD OF EXAMINERS

1. _____

Dr. M. Ali Asgar (Supervisor) — Chairman
Professor
Department of Physics, BUET, Dhaka

2. _____

Dr. Md. Abu Hashan Bhuiyan — Member
Professor
Department of Physics, BUET, Dhaka

3. _____

Dr. Nazma Zaman — Member
Professor & Head — (Ex- officio)

Department of Physics, BUET, Dhaka

4. _____

Dr. Farid Uddin Ahmed — Member
Chief Scientific Officer — (External)
Director, Physical Science Division
Bangladesh Atomic Energy Commission
Dhaka.

CANDIDATE'S DECLARATION

It is hereby declared that this thesis or any part of it has not been submitted elsewhere for the award of any degree or diploma.

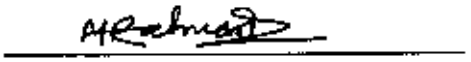

Md. Mustafizur Rahman

CONTENTS

"List of Tables"

"List of Figures"

ACKNOWLEDGEMENTS

I am extremely delighted to express my indebtedness and deep sense of gratitude to my Supervisor Professor Dr. M. Ali Asgar, Department of Physics, Bangladesh University of Engineering and Technology, Dhaka, for suggestion and inspiration which allowed me to complete this thesis.

I am grateful to Dr. Nazma Zaman, Head, Department of Physics, Bangladesh University of Engineering and Technology, Dhaka, for her official co-operation. I am grateful to Professor Mominul Huq of the same department for his valuable advice during the work.

I expressed my gratitude to Dr. Md. Feroz Alam Khan, Department of Physics, BUET, for his generous help in the Laboratory.

I am grateful to Professor Md. Abu Hashan Bhuiyan, Department of Physics, BUET, Dhaka, for his co-operation. I would like to offer my thanks to Dr. Jibon Podder.

I am specially grateful to Md. Israil Hossain, Scientific Officer, RRI, Faridpur, for his great inspiration and co-operation.

I expressed my gratitude to my parents, brother, sister and to my friends for their encourage in keeping my spirits high.

I also want to express my gratefulness to the authority of BUET for giving me the opportunity to do this research and financial support.

Thank you all.

Md. Mustafizur Rahman

ABSTRACT

Ferrite samples were prepared with new compositions $Ni_{0.5-x}Zn_{0.5}Co_xFe_2O_4$ [x = 0.2, 0.3, 0.4, 0.5], $Mn_{0.5-x}Zn_{0.5}Co_xFe_2O_4$ [x = 0.2, 0.3, 0.4, 0.5].

The diameter and thickness of the prepared samples were 11 mm and 2mm respectively.

The crytallinity of these samples has been checked by x-ray diffraction technique. Magnetostriction of these pallets has been measured by resistance straingauge technique at room temperature as a function of Magnetic field with different compositions. The linear saturation Magnetostriction of the pallets has been determined by rotating the magnetization vector from perpendicular position to parallel position of the magnetization direction with respect to the direction of strain measurement. It is assumed that the direction of the field and the direction of the magnetization practically coinsides, specially for the maximum field. The direction of measurement of strain is determined from the direction of the bonded straingauge. The Magnetostriction in crystals originate from the Magnetoclastic interaction associated with the local anisotropies and the local strain controlling the local direction of the magnetic moments. The saturation magnetostriction decreases as Ni-concentration increases. On the other hand the saturation magnetostriction increases as Mn concentration increases. The magneto elastic energy and hence magnetostriction depends on the electrons located at the Fermi level of the ferrite and is proportional to the spin-orbit energy shift at the Fermi level. However, the result has been compared with existing localized model of magneto elastic interaction. The results are interpreted in terms of domain motion and domain rotation, which are spontaneously strained.

We have also measured thermal expansion of these ferrites by using straingauge technique at liquid Nitrogen temperature to room temperature without Magnetic field. The measured linear thermal expansion coefficient are correlated with the results of previous workers.

CHAPTER - I

INTRODUCTION

CHAPTER I

INTRODUCTION

1. Introduction

Ferrite is a well known Ferrimagnetic material with various applications in magnetic devices. Its magnetic characteristics like magnetization, curie temperature, coercive force quarcive force and complex permeability have been studied for various compositions [1.1, 1.2]. However, magnetostriction of Ferrites which play an important role in determining the magnetic softness by affecting of domain organization, domain rotations and domain wall motions is relatively much less studied specially as a function of composition and temperature. Ferrite has many interesting aspects yet unexplored from the point of view of theoretical understanding and development of characteristics, arising from compositional variation for special applications.

The objectives of the present work is to prepare ferrite samples with new compositions $Ni_{0.5-x}Zn_{0.5}Co_xFe_2O_4$ [x=0.2, 0.3, 0.4, 0.5], $Mn_{0.5-x}Zn_{0.5}Co_xFe_2O_4$ [x = 0.2, 0.3, 0.4, 0.5]. for its magnetic characteristics that are favourable for applications as soft magnetic materials. Since magnetic softness, as reflected in permeability is determined by magnetic moment, magnetostriction and magnetic anisotropy, the compositional dependence of magnetostriction will be studied to understand the mechanism involved in producing magnetoelastic effects in ferrites. The temperature and composition dependence of the series will be investigated in order to find the optimum compositions which correspond to maximum and minimum magnetostriction [1.3, 1.4, 1.5]. Materials with high magnetostriction are important technologically for making magnetostrictive transducers and for producing permanent magnets while materials with low magnetostriction is used for soft magnetic materials. The magnetization and magnetostriction measurements of these ferrites will be performed and the results will be correlated. The variation of magnetostriction with temperature and composition will be studied to check the spin-orbit interaction mechanism localized model as the origin of

magnetostriction [1.6.,1.7]. Thermal expansion of these ferrites will be measured specially around the magnetic transition to find the magnetic contribution to lattice energy and hence spontaneous magnetostriction from the possible thermal expansion anomaly [1.8] would be measure very careful. However dne to the lack of high temperature strain gauges, the thermal expansion measurement have been carried out in the low temperature range down to liquid nitrogen temperature.

NiZn and MnZn ferrites of different compositions by partially substituting Co for Ni and Mn have been prepared by solid-state reaction. Optimum sintering temperature was determined by trail and error method for the desired solid-state reaction and homogeneity of the specimens [1.9]. It was checked by x-ray diffraction.

A whetstone bridge in out of balance condition has been used for measuring the thermal expansion and magnetostriction of ferrite samples [1.10, 1.11]. The dummy gage has been used on a fused silica, while the active gauge has been bonded on the sample to be studied in the form of a disk for minimum demagnetizing effect. Micromeasurement straingages have been nsed for determining saturation magnetostriction, from the measurement of magnetostrictive strains in the specimens as functions of magnetic field strengths and direction of magnetostriction [1.12, 1.13]. The results have been compared with the existing localized model of magneto elastic interaction [1.14]. The spontaneous magnetostrictions of the specimens will be obtained from the possible thermal expansion anomalies at the ferrimagnetic ordering temperature [1.15].

The results of thermal expansion and magnetostriction are discussed in chapter VI.

CHAPTER - II

Theory of Thermal Expansion

2.1 Introduction
2.2 Methods of Measurement of thermal expansion solids
2.3 Microscopic Measurements
2.4 Advantages
2.5 Strain Gage Technique
2.6 Lattice Contribution to Thermal Expansions
2.7 Electronic and Magnetic Contribution to Thermal Expansion

CHAPTER II
THEORY OF THERMAL EXPANSION

2.1 Introduction:

Thermal expansion is an important and common phenomena. In crystal it has important applications in modern equipment, where thermal changes occur. A short discussion on the mechanism of thermal expansion is given below.

Thermal expansion of a solid is a direct consequence of the anharmonicity of lattice vibrations. It, therefore, provides a convenient measure of the anharmonic parameters in a crystal. The anisotropy of thermal expansion is clearly exhibited if measurements are made on a single crystal. The expansion of a crystal when it is heated is a direct manifestation of the anharmonic nature of the inter-atomic forces in solids. If the forces were purely harmonic the mean positions of the atoms would not change even though the atoms would vibrate with larger and larger amplitudes as the temperature increases. While the temperature variation of the specific heat of solids was quite well understood with the development of the Born-von Karman's theory[2.1] of lattice vibrations in crystals, there was little attempt to calculate the thermal expansion of crystals in any detail till recent time. This was partly because of the paucity of experimental data on the thermal expansion of crystals below room temperature.

While Gruneisen's theory[2.2] of thermal expansion provided a general explanation of the phenomenon on the quasi-harmonic approximation, a detailed study of the temperature variation of thermal expansion below room temperature was started only after the work of Barron[2.3] in 1955. The theoretical study provided an impetus to the development of refined experimental techniques to measure the thermal expansion of crystals down to liquid helium temperature. The techniques so developed are sensitive enough to measure a change in length of the specimen of a fraction of an Angstrom. A large body of reliable data has been accumulated on a variety of simple crystals in which

the forces of interaction are fairly well understood. A fairly satisfactory explanation has been provided for the temperature variation of the thermal expansion in these simple solids on the quassi harmonic theory. These review deals with the progress achieved both in the theoretical and experimental study of thermal expansion in recent times. The linear thermal expansion coefficient α of a solid is defined as the increase in tenth suffered by unit length of the solid when its temperature is raised by a degree celsius. The limiting value of the ratio $\frac{1}{l_T}\frac{\delta l}{\delta T}$ as the increase in temperature $\delta T \rightarrow O$ is defined as the true expansion coefficient of the solid. Usually it is mean coefficient of expansion measured. A similar definition holds for the volume expansion coefficient β, of the solid. The volume expansion coefficient of the solid is related to its linear expansion coefficient.

A solid can be crystalline or amorphous an example for the latter being glass. We are concerned only with crystalline solids. These are available in two forms; single crystals formed by the monotonous repetition in space of a simple structural unit according to definite laws of symmetry; or polycrystalline material composed of small crystallites oriented in all possible directions. It is needless to emphasize that for any theory of the solid state a study of single crystals is of great importance, polycrystalline material introduces great complesities in the understanding of the physical processes involved. As an examples, mention may be mode of calmium and zinc where a study of the expansion of polycrystalline material yielded widely divergent results. This confusion was cleared up when single crystals of these substance were studied.

The measurement of thermal expansion of crystals is of importance for the following reasons:

1. The expansion coefficient is a structure sensitive property and reflects any transitions in crystal structure.

2. Knowledge of thermal expansion at low temperature is useful to isolate the electronic and the nuclear hyperfine contributions to the Gruneisen's parameter from the lattice contribution.
3. A knowledge of lattice thermal expansion of a material is essential in investigations involving epitaxy and thin film growth and in thinfilm deposition in industry.

2.2 Methods of Measurement of Thermal Expansion of Solids:

Various methods of measurement of thermal expansion are discussed briefly here. On the basis of the physical principle involved in the measurements, the different methods can be classified under two general headings; (i) Microscopic (lattice) expansion measurements and (ii) Macroscopic methods, where the average linear change of the bulk material.

The observations on thermal expansion can be made using either a static procedure or a dynamic procedure.

In the static procedure the temperature of the material under investigation is maintained constant for a certain interval of time, and the variation of the length that takes place during the passage from one temperature to the other is measured successively. The measurement is thus carried out between two different conditions of thermal equilibrium, and this leads to an accurate knowledge of the variation of length with temperature. On the other hand in the dynamic procedure the temperature of the specimen is varied continuously, and indirect observations on the variations of the length of the specimen are made simultaneously. This procedure is less cumbersome than the static method. However, the temperature in the interior of the specimen may not be uniform, and the results obtained thereby may not be very accurate unless the variation of temperature is maintained at a very low rate.

2.3 Microscopic Measurements

The lattice constants of solids are usually determined using x-ray diffraction techniques with the help of Brag's relation

$$n\lambda = 2d\,Sin\theta \qquad 2.3.1$$

where λ is the wavelength of the incident beam of x-rays and θ is the glancing angle for a given reflection. In practice, only first-order reflections (n =1) are considered. The alteration in the distance between the atomic planes or the lattice spacing d, consequent to the expansion of the solid when the temperature is altered will be reflected as a change in the parameter 0. From the Bragg's law, we get

$$\frac{\Delta d}{d} = \frac{\Delta \lambda}{\lambda} - \Delta\theta.\cot\theta \qquad 2.3.2$$

For a closely constant spectral distribution $\Delta\lambda \approx 0$, and for large θ, the shift in augle Δ0, becomes a sensitive measure of lattice expansion. Therefore equation (2.3.2) becomes

$$\frac{\Delta d}{d} = -\Delta\theta.\cot\theta \qquad 2.3.3$$

2.4 Advantages

The x-ray method has the following advantages over the other methods in dilatometry to be described later. They are

(i) It is an absolute method for determination of the value of α, whereas most other methods make use of a reference standard at the temperature of the specimen.

(ii) A single experiment yields complete information on the expansion coefficient along various directions in an anisotropic crystal.

(iii) The sensitivity of measurements in $\frac{\Delta d}{d}$ of about 4×10^{-6} will be maintained down to temperature of $H_D/10$.

2.5 Stain gauge Technique

In microscopic measurement, x-ray diffraction method is good technique to measure thermal expansion of solids. But to measure the thermal expansion we have used strain gange technique. Usually strain gauge technique is used for magnetostriction measurement. But this strain gauge technique has been used for thermal expansion at low temperature, for the first time by E.W. Lee and M. A. Asgar [2.4] for determining anamolous thermal expansion. Although it is an indirect method but it has the advantage over x-ray technique of quite high sensitivity and can be used for directional measurement. However disadvantage of this method is the non availability of strain gauge that can be used at high temperature.

2.6 Lattice Contribution to Thermal Expansion

The normal modes of vibration of a crystal lattice are plane waves in the harmonic approximation. Each Wave is characterised by a waves vector 'q' and a frequency $\omega(q)$. If there are p atoms in the unit cell of the crystal, there are 3p different normal modes denoted by the index j running from 1 to 3p. Of the 3p branches $\omega_j(q)$, there are 3 branches, j = 1,2,3 which correspond to the elastic waves propagated in the lattice in the limit of long wavelengths ($q \to o$). In this limit of long waves, the different atoms in the unit cell move in unison in these modes. The remaining 3p-3 branches are celled optical branches. In the long wave limit, these modes of vibration correspond to the motion of the p sublattice one against the other. These are the frequencies which appear in the Raman and Infrared absorption spectra of the crystal. When we deal with a finite crystal having N unit cells the boundary conditions allow only N values of the wave vector $\bar{q}$ in the Brillouin zone. These allowed wave vectors are denoted by a subscript i to q. There are, therefore, 3pN normal modes of oscillation of the crystal lattice with frequencies $\omega_j(q_i)(j=1,.....,3p;\ i = 1, ..., N)$.

In the harmonic approximation there can be no thermal expansion. The atoms vibrate about their equilibrium positions symmetrically whatever be the amplitude. To account for thermal expansion one has to take into account the anharmonicity of the lattice vibrations. The simplest and most convenient way to do this is to assume that the harmonic approximation is valid for every volume of the crystal, bnt the frequencies of vibration are dependent on the volnme. This apoproximation is called the quasi-harmonic approximation and can be used as long as the temperature $T \leq \cup$, where $\cup$ is the equivalent Debye temperature of the crystal. The quasi-harmonic approximation provides the most convenient method for disenssing the thermal expansion of a crystal at moderate temperatures. The reason for the success of the qnasi-harmonic approximation will be disenssed in a later section. The first detailed theoretical discussion of thermal expansion on this basis was given by Barron. Barron's work stimulated considerable experimental and theoretical research in the last decade on the thermal expansion of crystal.

In the quasi-harmonic approximation a normal mode of frequency $\omega_j(q_i)$ has a free energy associated with it. This free energy $f_{j,i}$ is given by

$$\mathrm{fj,i} = \mathrm{kT}\{\tfrac{1}{2}\mathrm{xj,i} + \mathrm{In}[1 - \exp(-\mathrm{xj,i})]\} \qquad 2.6.1$$

where k is the Boltzmann's constant, T is the temperature in degrees Kelvin and

$$x_{j,i} = h\omega_j\left(\bar{q}_i\right)/kT \qquad 2.6.2$$

where h is the Planck's constant.

The total free energy $\Im$ (T,V) due to all the normal modes of vibration is given by

$$\begin{aligned}\Im(T,V) &= \sum_{j=1}^{3n}\sum_{i=1}^{N} f_{j,i} \\ &= kT\sum_{j=1}^{3n}\sum_{i=1}^{N}\left\{\frac{1}{2}x_{j,i} + In\left[1-\exp\left(-x_{j,i}\right)\right]\right\}\end{aligned} \qquad 2.6.3$$

This is a function of temperature and volnme. Using the thermodynamic relation

$$S = -\frac{\partial \Im}{\partial T}\Big)_v \qquad 2.6.4$$

for the entropy, we get

$$S = k\sum_{j=1}^{3p}\sum_{i=1}^{N}\left\{\frac{x_{j,i}\exp(-x_{j,i})}{[1-\exp(-x_{j,i})]} - ln[1-\exp(-x_{j,i})]\right\} \qquad 2.6.5$$

The specific heat at constant volume C_{vhar} in the harmonic approximation is

$$C_{vhar} = T\frac{\partial S}{\partial T}\Big)_v = k\sum_{j=1}^{3p}\sum_{i=1}^{N}\sigma_{j,i} \qquad 2.6.6$$

where

$$\sigma_{j,i} = x_{j,i}^2\exp(x_{j,i})/[1-\exp(x_{j,i})]^2 \qquad 2.6.7$$

is the Einstein specific heat function.

From the thermodynamic relation

$$\frac{\partial S}{\partial T}\Big)_I = \frac{\partial P}{\partial T}\Big)_v = \frac{\beta}{\chi_T} \qquad 2.6.8$$

where P is the pressure, β is the volume expansion coefficient and χ_t is the isothermal compressibility we obtain

$$\frac{\beta V}{\chi_T} = k\sum_{j=1}^{3p}\sum_{i=1}^{N}\gamma_{j,i}\sigma_{j,i} \qquad 2.6.9$$

where

$$\gamma_{j,i} = -\frac{\partial\, ln\, x_{j,i}}{\partial\, ln V} = -\frac{\partial\, ln\, \omega_j(q_i)}{\partial\, ln V}$$

$\gamma_{j,i}$ is called the Grüneisen parameter for the normal mode frequency $\omega_j(q_i)$.

This represents the fractional change in the frequency with the fractional change in volume. In the quasi-harmonic approximation the $\gamma_{j,i}$ are non-zero in general and are

assumed to be independent of volume and temperature. This latter assumption is not quite justified.

The temperature dependenced of the volume expansion coefficient can be expressed most conveniently in terms of the temperature dependence of an equivalent Grüneisen parameter γ_T defined by the relation

$$y_{j,i} = -\frac{\beta V}{\chi_T C_{vhar}} \qquad 2.6.10$$

γ_T is, therefore, the weighted average over the Grüneisen parameters for the individual normal modes.

Grüneisen (2.5) stated his law that $\beta V/\chi_T C_v$ is constant, independent of temperature. This law is found to be approximately valid at moderately high temperatures. Grüneisen's law would be strictly valid at all temperature if the Grüneisen parameters $y_{j,i}$ for all the modes of lattice vibration were equal. This is improbable. In fact even for the simple Debye model of an isotropic elastic continuum, the longitudinal and transverse elastic waves would have different Grüneisen parameters leading to a temperature dependence of γ_T (2.6). However, eqnality of all the Grüneisen parameters is not necessary for a solid to obey Grüneisen's law. Blackman has pointed ont that the variation of γ_T can be considered from a different point of view. One constructs constant frequency surfaces ω and $\omega + d\omega$ in the Brillouin zone. The average Grüneisen parameter $y(\omega)$ is defined by taking the average of the Grüneisen parameters of the individual modes in this frequency region γ_T can now be redefined as

$$y_r = \frac{\int_0^{\omega_m} y(\omega).\sigma(\omega).G(\omega).d\omega}{\int_0^{\omega_m} \sigma(\omega).\bar{G}(\omega).d\omega} \qquad 2.6.11$$

where $\sigma(\omega)$ is the Einstein specific heat function and $G(\omega)$ is the frequency distribution function for the lattice. Though the individual Grüneisen parameters $y_{j,i}$ for the different

normal modes may be widely different, the average $\gamma(\omega)$ may not depend strongly on the frequency. This is the reason why γ_T shows a much smaller range of variation than the $\gamma_{j,k}$.

If it so happens that $\gamma(\omega)$ is independent of frequency then γ_T will be independent of temperature. Then the solid obeys the Grüneisen's law over the entire temperature range. Such a solid is called a perfect Grüneisen solid. This is as far as the general theory of thermal expansion.

2.7. Electronic and Magnetic Contribution to Thermal Expansion

In a metal the total contribution to the entropy arises from lattice vibrations, conduction electrons and magnetic interactions. If we write the entropy as

$$S = S_l + S_E + S_m \qquad 2.7.1$$

then the specific heat is given by

$$C_v = T\frac{\partial S}{\partial T}\Big)_v = C_{el} + C_{ve} + C_{vm} \qquad 2.7.2$$

The thermal expansion is given by the relation

$$\frac{\partial S}{\partial V}\Big)_T = \frac{\partial S}{\partial T}\Big)_v = \frac{\beta}{\chi} \qquad 2.7.3$$

If the different contributions to the entropy are functions $S_i(O_i/T)$ where $)_i$ is a characteristic temperature, then

$$\frac{\partial S}{\partial V}\Big)_T = \frac{\gamma_i C_{vi}}{V} \qquad 2.7.4$$

where

$$\gamma_i = -\frac{V}{H_i}\cdot\frac{\partial H_i}{\partial V}\Big)_T \qquad 2.7.5$$

is the corresponding Grüneisen parameter. We could, therefore, write

$$\beta = \frac{\chi_T}{V}(\gamma_l C_{vl} + \gamma_e C_{ve} + \gamma_m C_{vm} \qquad 2.7.6$$

It is well known that the conduction electrons in a metal contribute a term to the specific heat proportional to the temperature T. So we should expect in a metal a contribution to thermal expansion coefficient from the conduction electrons which would be linear in temperature. At low temperatures where the lattice contribution to the expansion coefficient varies as T^3, we could write α as

$$\alpha = BT + DT^3 \qquad 2.7.7$$

By plotting α/T against T^2 the values of B and D can be found. From the value of B and the measured electronic specific heat one could obtain the value of γ_e.

Varley (1110) has derived the following theoretical expression for γ_e.

$$\gamma_e = 1 + \frac{\partial \ln D(E_F)}{\partial \ln V}\Big)_{E_F} - \frac{N}{n^2(E_F)}\cdot\frac{\partial n(E_F)}{\partial E_F}\Big)_V\left[1 + \frac{\partial \ln N}{\partial \ln V}\Big)_{E_F T}\right] + \frac{C_{ve}}{\beta V n^3(E_F)}\cdot\frac{\partial n^2(E_F)}{\partial E_F}\Big)_V \qquad 2.7.8$$

Here $n(E_F)$ is the number density of states per unit volume at the Fermi level E_F; N is the total number of conduction electrons per unit volume in the metal. For a single band free electron model $n(E_F)$ depends only on E_F and

$$\frac{N}{n^2(E_F)}\cdot\frac{\partial n(E_F)}{\partial E_F} = \frac{1}{3} \qquad 2.7.9$$

γ_e for such a case should be 2/3. Where the single band free electron model is not applicable the value of γ_e can be very different from 2/3. The magnitude and sign of γ_e will depend on: (1) how rapidly and in what direction $n(E_F)$ varies with energy at the Fermi level; and (2) how sensitive $n(E_F)$ is to change in volume V. In exceptional cases the electronic Grüneisen parameter could be negative yielding a negative contribution to the thermal expansion coefficient.

In ferromagnetic materials at the Curie temperature and in antiferromagnetic materials at the Néel temperature the onset of ordering of the spins is accompanied by an anomaly in thermal expansion. This effect has been observed in many cases. In such ordered spin arrays at very low temperatures there could be excitations involving spin reversal on a

few of the atoms. These excitations are called spin aves and when quantized these elementary excitations go under the name of magnons. It is well known (2.7) that in ferromagnetic and ferrimagnetic materials these spin waves obey a quadratic dispersion law: ($\omega(q) \propto q^2$) and yield a magnon contribution to the heat capacity varying as $T^{3/2}$ at low temperatures. This magnon contribution to the heat capacity has been observed by Shinozaki (2.8) in Yttrium iron garnet (YIG) and Kouvel (2.9) in magnetic. In ferromagnetic metals this contribution is superposed on the electron contribution to the specific heat and it becomes difficult to separate the two effects. In ferrimagnetic materials the electronic contribution is absent and the magnon contribution can be easily detected. Magnons must also contribute to the thermal expansion of these materials. Oue would expect a similar contribution to the thermal expansion in the antiferromagnetic materials. There are no experiments so far on the magnon contribution to thermal expansion in ferro, ferri, and antiferro-magnetic materials.

CHAPTER - III

Magnetostriction

3.1 Phenomenology of Magnetostriction
3.2 Physical Origin of Magnetostriction
3.3 Mechanism of Magnetostriction
3.4 Magnetostriction in Polycrystal
3.5 Direction of Linear Magnetostriction
3.6 Magnetostriction Arising from Domain Rotation

CHAPTER III
MAGNETOSTRICTION

3.1 Phenomenology of Magnetostriction

Magnetostriction is that phenomenon wherein the lattice of a ferromagnetic specimen changes during the process of magnetization. The deformation $\delta l/l$ due to magnetostriction is as small as $10^{-5} \sim 10^{-6}$. Such a deformation can be conveniently be measured by means of a strain gauge technique the details of which are described later.

The strain due to magnetostriction changes with the increase of the magnetic field intensity as shown in figure (3.1) and finally reaches the saturation value λ.

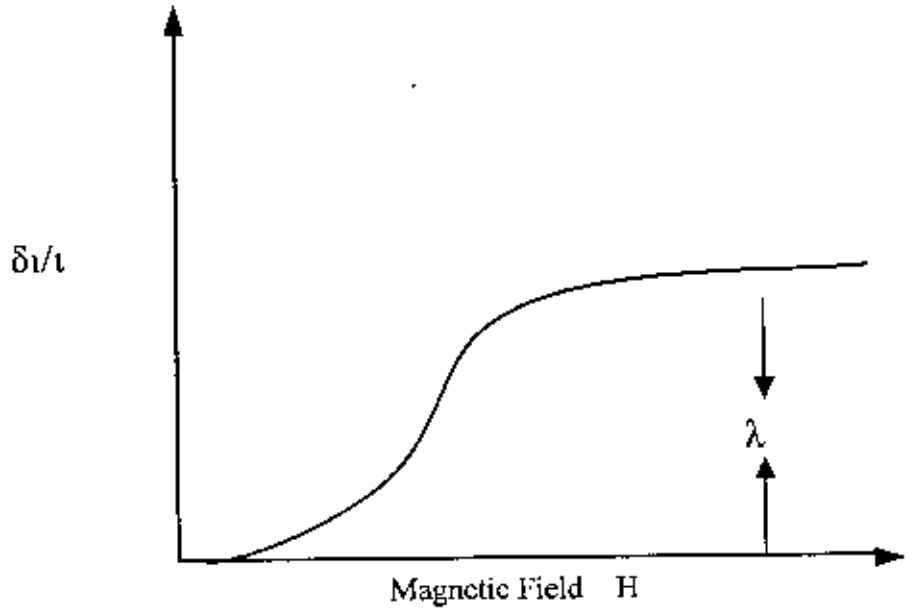

Fig. 3.1: Magnetostriction as a function of the field intensity

The reason is that the crystal lattice inside each domain is spontaneously deformed in the direction of domain magnetization and its strain axis rotates with a rotation of the domain magnetization, thus resulting in a deformation of the specimen as a whole (Fig. 3.2). In order to calculate the dependence of the strain on the direction of magnetization we consider a ferromagnetic sphere, which is a real sphere only when it is demagnetized but is elongated by $\delta l/l = e$ in the direction of magnetization after it is magnetized (Fig. 3.3). The elongation of a diameter of the sphere along a direction which makes an angle φ with the direction of magnetization is given by

$$\frac{\delta l}{l} = e\cos^2\phi \qquad 3.1$$

when the domain magnetizations are distributed at random in a demagnetized state as shown in figure 3.2a, the average deformation is given by the average of (3.1); thus

$$\left(\frac{\delta l}{l}\right)_{demag} = \int_0^{\pi/2} e\cos^2\phi \sin\phi\, d\phi = \frac{e}{3} \qquad 3.2$$

Since, in the saturated state, as shown in figure 3.2b

$$\left(\frac{\delta l}{l}\right)_{sat} = e \qquad 3.3$$

the saturation magnetostriction is given by

$$\lambda = \left(\frac{\delta l}{l}\right)_{sat} - \left(\frac{\delta l}{l}\right)_{demag} = \frac{2}{3}e \qquad 3.4$$

Thus the spontaneous strain in a domain can be expressed in terms of λ as

$$e = \frac{3}{2}\lambda \qquad 3.5$$

We assumed above that the magnitude of the spontaneous strain is independent on the crystallographic direction of magnetization. In this case we have to do with an isotropic magnetostriction.

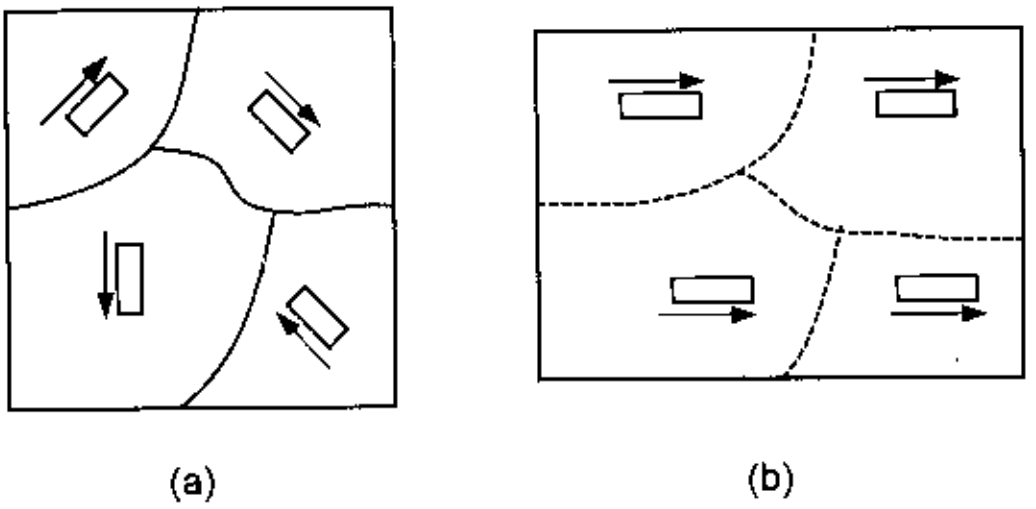

Fig. 3.2: Rotation of domain magnetization and accompanying rotation of the axis of spontaneous strain.

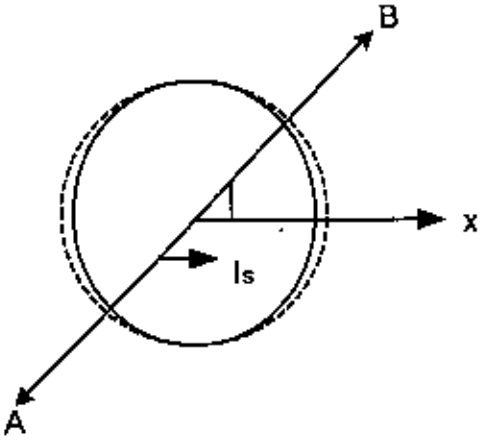

Fig. 3.3 Observation of elongation in a direction which makes an angle ϕ with the axis of spontaneous strain.

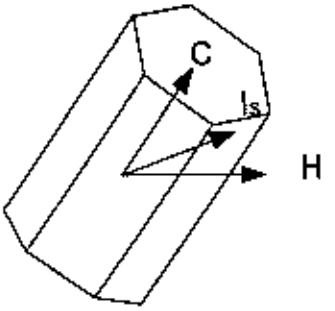

Fig. 3.4 Magnetization of a uniaxial crystal

Next we discuss how the magnetostrictive elongation changes as a function of intensity of magnetization. First we consider ferromagnetic substance, such as cobalt, with a uniaxial anisotropy. If the magnetic field H makes an angle ψ with the easy axis (Fig. 3.4), the magnetization takes place by the displacement of 180^0 walls untill the magnetization reaches the value $\cos\psi$; during this process no magnetostriction can be observed. Then the domain magnetization rotates towards the direction of the applied field. During this process the elongation changes by the amount

$$\Delta\frac{\delta l}{l}=\frac{3}{2}\lambda\left(1-Cos^2\varphi\right) \qquad 3.6$$

If H is parallel to the easy axis, that is if $\psi = 0$, (3.6) give $\Delta\frac{\delta l}{l}=0$; in other words, there is no change in the length of the specimen from the demagnetized state to saturation. On the other hand, if H is perpendicular to the easy axis, that is if $\psi = \pi/2$, (3.6) gives $\Delta\left(\frac{\delta l}{l}\right)=\frac{3}{2}\lambda$.

The change in $\frac{\delta l}{l}$ is shown graphically in figure 3.5 as a function of magnetization for various values of ψ. For a polycrystal if we assume that all wall displacements are finished before the onset of rotation magnetization, we have, simply by averaging the above values,

$$\psi / \bar{\psi}, I=\frac{Is}{2}, \Delta\left(\frac{\delta l}{l}\right)=\lambda \qquad 3.7$$

The $\frac{\delta l}{l}$ vs I relation for this crystal is shown by the dotted curve in figure 3.5.

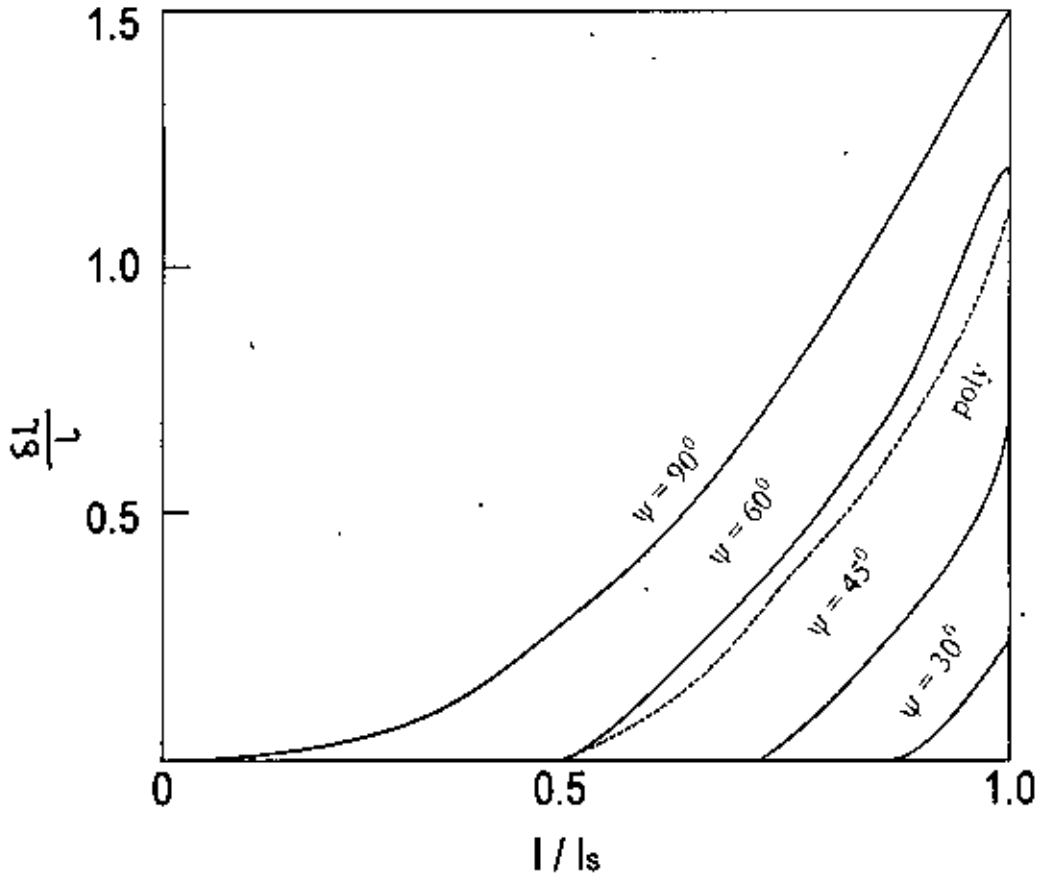

Fig. 3.5: Magnetostriction of a uniaxial ferromagnetic crystal as a function of the intensity of magnetization

The magnetization is along one of the <100> directions in each domain, so that the average elongation of the demagnetized specimen is given by $\left(\frac{\delta l}{l}\right)_{dem} = \lambda/2$ regardless of the direction of observation. If this crystal is magnetized to its saturation parallel to [100]

$$\left(\frac{\delta l}{l}\right)_{sat} = \frac{3}{2}\lambda$$

so that

$$\Delta\left(\frac{\delta l}{l}\right)_{van} = \left(\frac{3}{2}\lambda\right) - \lambda/2 = \lambda \qquad 3.8$$

For the case of polycrystal $\lambda_{100} = \lambda_{111} = \lambda$, we got the same result, that is

$$\Delta\frac{\delta l}{l} = \left(\frac{3}{2}\lambda\right) - \lambda/2 = \lambda \qquad 3.9$$

3.2 Physical Orgin of Magnetostriction

Magnetostriction which is commonly defined as any change in dimensions of a body caused by a change in its magnetic states is a property which can be considered as being among the most important intrinsic materials parameter. The Physical origins of magnetostriction is explained along the following lines[3.1].

For non S-state ions the orbital angular momentum has non-zero value of L with (2L+1) degeneracy in the lowest energy ground state. The orbital charge distribution for the ions is highly asymmetric. When these paramagnetic ions are surrounded by crystalline electrical field within a crystal, the orbital degeneracy is removed and the resultant wave function form new linear combinations, which reflect the local symmetry of the crystal. The rotation of the charge distribution lobes alters the orbital angular momentum, because of spin orbit coupling. The magnetization associaqted with spin will thus be related.

Spin-orbit coupling also contributes to the anisotropy by way of another mechanism called anisotropic exchange introduced by van vleck [3.2]. For S-state ions the orbital angular momentum is zero and the charge distribntion is somewhat distorted by the crystal field. The spin-orbit coupling thus contributes to the anisotropy energy and the magnetostriction in this case as well, although of much smaller magnitude. Exchange energy can make contribuitions to magnetoclastic energy due to the strain dependence of

the exchange integral J_{ij}. When the magnetic moments of neighbouring ions are rotated away from parallelism. The exchange energy while increasing the elastic energy gives rise to magnetostriction and the origin of the local strains have been discussed in terms of the single-ion model with random local axis *[3.3], [3.4], 3.5], 3.6], [3.7], [3.8], [3.9], [3.10], [3.11], [3 12], [3.13], [3.14], [3.15].*

There are three mechanism of anisotropy

(i) Crystal field anisotropy

(ii) Exchange anisotropy and

(iii) Exchange striction

which is shown schematically in figure (3.6a), (3.6b) and (3.6c) respectively

3.3 Mechanism of Magnetostriction

The origin of magnetostriction along the lines of Neel's [3.16] theory, which was developed in this paper on magnetic annealing and surface anisotropy, is as follows.

When the distance between the atomic magnetic moments is variable, the interaction energy is expressed by

$$W(r,Cos\Phi)=g(r)+I(r)\left(Cos^2\Phi-\frac{1}{3}\right)+q(r)\left(Cos^4\Phi-\frac{6}{7}Cos^2\Phi+\frac{3}{35}\right)+\ldots\ldots\ldots \quad 3.10$$

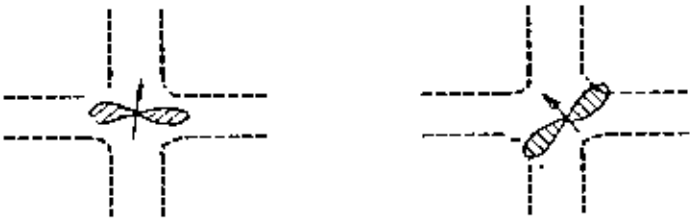

(a) Crystal Field Anisotropy

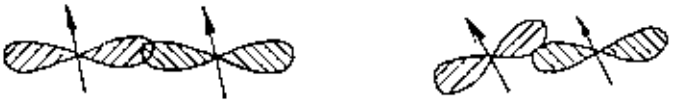

(b) Exchange Anisotropy

(c) EXCHANGE STRICTION

Fig. 3.6: Physical Origin of Magnetostriction

If the interaction energy is a function of r, the crystal lattice must be deformed upon the generation of a ferromagnetic moment, because such interaction tends to change the bond length in a different way depending on the bond direction. The first term g(r) is the exchange interaction term and is of relevance only when volume magnetostriction is considered as manifested in thermal expansion anomaly at the magnetic ordering temperature.

If α denotes the direction of domain magnetization and that of the bond direction, we can write

$$W = g(r) + 1(r)\left\{(\alpha_1\gamma_1 + \alpha_2\gamma_2 + \alpha_3\gamma_3)^2 - \tfrac{1}{3}\right\} + q(r)\left[(\alpha_1\gamma_1 + \alpha_2\gamma_2 + \alpha_3\gamma_3)^4 - \tfrac{6}{7}(\alpha_1\gamma_1 + \alpha_2\gamma_2 + \alpha_3\gamma_3)^2 + \tfrac{3}{35}\right] + \ldots\ldots\ldots \quad 3.11$$

Considering a deformed cubic lattice and relating the direction cosines γ_1 to the strain tensor L_{ij}, we can get the expansion for magnetoclastic energy. Science the magnetoelastic energy has a linear dependence on strain the crystal will deform without limit unless it is counter balanced by the elastic energy which increases rapidly because of its quadratic depencence on strain.

By differentiating, the total energy = $E_{mag\ elastic} + E_{elastic}$
with respect to the strain components, and setting the partial derivatives equal to zero, for minimum energy condition, one can obtain the relation for the fractional change in length of the crystal in any arbitrary direction β as

$$\lambda = \sum_{i,j=1} e_{ij}\beta_i\beta_j \quad 3.12$$

Substituting the values of strain components as obtained by minimizing total energy coming from magnetoclastic and elastic terms, we can get an expression for

$$\lambda_\beta = h_o + h_1\left(\sum_{i,j}^{2}\beta_i^2 - \frac{1}{3}\right) + 2h_2c_{ij}(\alpha_i\alpha_j\beta_i\beta_j) + h_3 s + h_4\left(\sum\alpha_1^4\beta_j^2 + \frac{2}{3}s - \frac{1}{3}\right) + 2h_5c_{ij}\left[\alpha_i\alpha_j\left(1 - \alpha_1^2 - \alpha_i^2\right)\beta_i\beta_j\right] + \ldots\ldots\ldots\ldots \quad 3.13$$

where C_{ij} indicates a summation over terms with cyclic permulation of the indicies and $h_0 \rightarrow h_5$ are the magnetostriction constant defined by

$$h_0 = \frac{-b_o}{c_{11}+2c_{12}}, \qquad h_1 = \frac{-b_1}{c_{11}-c_{12}}$$

$$h_3 = \frac{-b_3}{c_{11}+2c_{12}}, \qquad h_4 = \frac{-b_4}{c_{11}-2c_{12}}$$

$$h_5 = \frac{-b_5}{2c_{44}} \qquad 3.14$$

where the coefficients b_n are magnetoelastic coupling coefficients.

For hexagonal crystals the relations become modified due to different symmetry conditions and have been treated in detail by Nason and Lewis[3.17].

For cubic crystals neglecting higher terms in the polynomial.

$$\lambda_\beta = \tfrac{3}{2}\lambda_{100}\left(\alpha_1^2\beta_1^2 + \alpha_2^2\beta_2^2 + \alpha_3^2\beta_3^2 - \tfrac{1}{3}\right) + 3\lambda_{111}\left(\alpha_1\alpha_2\beta_1\beta_2 + \alpha_2\alpha_3\beta_2\beta_3 + \alpha_3\alpha_1\beta_3\beta_1\right) \qquad 3.15$$

where λ_{100} and λ_{111} indicates strain along (100) and (111) direction respectively.

3.4 Magnetostriction in Polycrystal

In the case of polycrystalline magnetic material such that

$\lambda_{100} = \lambda_{111} = \lambda_s$

we get from equation (3.15)

$$\begin{aligned}\lambda_\beta &= \tfrac{3}{2}\lambda_s\left(\alpha_1^2\beta_1^2 + \alpha_2^2\beta_2^2 + \alpha_3^2\beta_3^2 - \tfrac{1}{3}\right) + 3\lambda_s\left(\alpha_1\alpha_2\beta_1\beta_2 + \alpha_2\alpha_3\beta_2\beta_3 + \alpha_3\alpha_1\beta_3\beta_1\right)\\ &= \tfrac{3}{2}\lambda_s\left[\alpha_1^2\beta_1^2 + \alpha_2^2\beta_2^2 + \alpha_3^2\beta_3^2 + 2\alpha_1\alpha_2\beta_1\beta_2 + 2\alpha_2\alpha_3\beta_2\beta_3 + 2\alpha_3\alpha_1\beta_3\beta_1 - \tfrac{1}{3}\right]\\ &= \tfrac{3}{2}\left[\left(\alpha_1\beta_1 + \alpha_2\beta_2 + \alpha_3\beta_3\right)^2 - \tfrac{1}{3}\right] \qquad 3.16\end{aligned}$$

$$\alpha_1\beta_1 + \alpha_2\beta_2 + \alpha_3\beta_3 = Cos\theta$$

where θ is the angle between the direction of magnetization and that of observation. When the domain magnetization rotates toward the direction of the applied field, the fractional change is given by

$$\lambda_\beta = \frac{\nabla 1}{1}$$

becomes from equation (3.16)

$$\frac{\nabla 1}{1} = \frac{3\lambda_s}{2}\left(Cos^2\theta - \frac{1}{3}\right) \qquad 3.17$$

3.5 Direction of Linear Magnetostriction

Experiments have shown that the deformation depends npon the direction of the magnetization. for a cubic crystal magnetize in the direction given by the direction cosines λ_1, λ_2 and λ_3 (defined with respect to the cubic axes). This deformation expressed in strain components ϵ_{ij} (i,j = x,y,z) become in first approximation.

$$\epsilon_{xx} = \frac{3}{2}\lambda_{100}\left(\alpha_1^2 - \frac{1}{3}\right)$$

$$\epsilon_{yy} = \frac{3}{2}\lambda_{100}\left(\alpha_2^2 - \frac{1}{3}\right)$$

$$\epsilon_{zz} = \frac{3}{2}\lambda_{100}\left(\alpha_3^2 - \frac{1}{3}\right) \qquad 3.18$$

$$\epsilon_{xy} = \frac{3}{2}\lambda_{111}\alpha_1\alpha_2$$

$$\epsilon_{yz} = \frac{3}{2}\lambda_{111}\alpha_2\alpha_3$$

$$\epsilon_{zx} = \frac{3}{2}\lambda_{111}\alpha_3\alpha_1$$

The extra terms $(-\frac{1}{3})$ make the total change of volume nil (trace of matrix is zero). The factors $-\frac{1}{3}$ ensure that the strain in the direction of magnetization with respect the non-magnetized state

$\left(\alpha_1^2 = \alpha_2^2 = \alpha_3^2 = \frac{1}{3}\right)$ is λ_{100} and -½λ_{111} in the [100] and [111] directions respectively. The strain in a direction perpendicular to λ_{100} and -½λ_{111} respectively.

In an arbitrary direction we then have parallel to the magnetization

$$\lambda_{(\alpha_1\alpha_2\alpha_3)} = \lambda_{100} + 3(\lambda_{111} - \lambda_{100})(\alpha_1^2\,\alpha_2^2 + \alpha_2^2\,\alpha_3^2 + \alpha_3^2\,\alpha_1^2) + \ldots\ldots\ldots \qquad 3.19$$

For the ferromagnetic materials the values of λ at room temperature are found to be

For iron

$$\lambda_{100} = +25 \times 10^{-6}$$

$$\lambda_{111} = -19 \times 10^{-6}$$

and for nickel

$$\lambda_{100} = -46 \times 10^{-6}$$

$$\lambda_{111} = -25 \times 10^{-6}$$

In discussing the effect of a unidirectional stress it is convenient to divide materials into two classes which have

(i) Positive magnetostriction

(ii) Negative magnetostriction

In materials of class (i) the magnetization is in increased by tension (except at I = 0 or I_s) and for the materials of class (ii) the magnetization is decreased by tension and the material contracts when magnetized.

3.6 Magnetostriction Arising from Domain Rotation

Magnetostriction is associated with domain orientation. The change in dimension of a single domain can be rotated in simple quantitative way to change in direction of magnetization in the domain as follows

$$\lambda_1 = \frac{3}{2}\lambda_s\left(Cos^2\theta - \tfrac{1}{3}\right) \qquad 3.20$$

Here θ is the angle between the direction in which the change in length is measured. It is assumed now that magnetostriction is independent of the crystallographic direction of magnetization and that the change in volume is zero. The zero point of λ_1 is chosen so that it is equal to the longitudinal change in length λ_s, where θ = 0 at saturation. When the length is measured at right angle to the direction of magnetization (transverse effect) $\theta = 90^0$ and the change in length

$$\lambda = -\lambda_{s/2}$$

For polycrystalline or amorphous material the domain are initially oriented at random. The same relation is applicable if one uses the average of $Cos^2\theta$ over all the domains. When the material is unmagnetized.,

$$\langle Cos^2\theta\rangle_{av} = \frac{1}{3} \; and \; \lambda = 0$$

Upon application of a strong field θ becomes zero and $\lambda = \lambda_s$.

If the domains are not initially random, one can use the relation

$$\lambda = \frac{3}{2}\lambda_s\left[\langle Cos^2\theta\rangle_{av} - \frac{1}{3}\right]$$

$$= \frac{3}{2}\lambda_s\left[\langle Cos^2\theta\rangle_{av} - \langle Cos^2\theta\rangle_o\right] \qquad 3.21$$

where $\langle Cos^2\theta\rangle_0$ = initial domain distribution

$\langle Cos^2\theta\rangle_{av}$ = domain distribution at any time

If the domain are oriented originally so that $\theta = 0$ for half of them and $\theta = 180^0$ for other half $\langle Cos^2\theta\rangle_0 = \langle Cos^2\theta\rangle_{av} = 0$ and $\lambda = 0$ (the reference point); in a strong field θ = 0 and there is no change in $Cos^2\theta$ and $\lambda = 0$. When used in this sense, λ depends decidedly on the initial domain distribntion while λ_s is a constant of the material. The constant λ_s

can be determined in any specimen by measuring λ when a saturation field is applied first parallel and then at 90^0 to the direction of measurement of λ. The total change in length caused by the change in the field in the polycrystalline or amorphous material is then

$$\frac{\nabla l}{l}=\frac{3}{2}\lambda_s \qquad 3.22$$

independent of the initial domain distribution.

CHAPTER - IV

Preparation of Ferrites

CHAPTER IV

PREPARATION OF FERRITES

4.1 Introduction

Ferrimagnetic oxides or ferrites as they are usually known, have become available as practical magnetic materials over the course of the last twenty years. During this time their use has become established in many branches of communication and electronic engineering and they now embrace a very wide diversity of compositions. Properties and applications. The scope of this book is restricted to the properties of those ferrites which are magnetically soft and which are of technical importance, and to the applications of such ferrites in devices which, in the broadest sense, may be described as inductors or transformers.

Magnetite, or ferrous ferrite, is an example of a naturally occurring ferrite. It hsa been known since ancient times and its weak permanent magnetism found application in the lodestone of the early navigators. Hilpert [4.1] in 1909 attempted to improve the magnetic properties of magnetite and in 1928 Forestier [4.2] preparaed ferrites by precipitation and heat treatment. Magnetic oxides were also studied by Japanese workers [4.3,4.4] between 1932 and 1935.

In 1936 Snoek [4.5] was studying magnetic oxides in Holland; by 1945 he had laid the foundations of the physics and technology of ferrites and new industry came into being [4.6].

Ferrites are ceramic materials dark grey or black in appearance and very hard and brittle. The magnetic properties arise from interactions between metallic ions occupying particular positions relative to the oxygen ions in the crystal structure of the oxide. In magnetite, in the first synthetic ferrites and indeed in the majority of present day

magnetically soft ferrites the crystal structure is cubic; it has the form of the mineral spinel. The general formula of the spinel ferrite is $MeFe_2O_4$ where Me usually represents one or, in mixed ferrites, more than one of the divalent transition metals *Mn, Fe, Co, Ni, Cu* and *Zn* or *Mg* and *Cd*. Other combinations, of equivalent valency are possible and it is possible to replace some or all of the travalent iron ions with other trivalent metal ions.

In the early practical ferrites Me represented *Cu+Zn, Mn+Zn*, or *Ni+Zn*. The first of these compound was soon abandoned and the other two, referred to as manganese zinc ferrite and nickel zinc ferrite were developed for a wide range of applications where high permeability and low loss were the main requirements [4,7]. These two compounds are still by far the most important ferrites for high permeability, low loss applications and constitute the vast majority of present day ferrite production. By varying the ratio of *Zn* to *Mn* or *Ni* or by othermeans, both types of ferrite may be made in a variety of grades, each grade having properties that suit it to a particular class of application. The range of permeabilities available extends from about 15 for nickel ferrite grades.

The applications started in the field of carrier telephony where the combination of good magnetic properties and high resistivity made these materials very suitable as cores for inductors and transformers. since the resistivities were at least a million times greater than the values for metallic magnetic materials, laminated or powdered cores could be replaced with solid ferrite cores and these could often be made in a more convenient shape than their laminated counterparts.

The application was extended to domestic television receivers where they became, and still remain, the undisputed core material for the line time base transformer and the magnetic yoke used in the deflection system. In domestic radio receivers, rods or plates of

ferrite are used as cores for magnetic antennas. Many other high permeability, low loss application have been found [4.8,4.9].

However, a short qualitative description of the spinel lattice, the magnetic domain and the magnetization process will be useful as a basis for the discussion of properties of ferrites.

4.2 Magnetism in Ferrites

4.2.1 The spinel lattice

Figure 4.1 shows a unit cell of the spinel lattice and the sites of the various ions. The small cubic diagram shows how the unit cell is composed of octants of alternate kind: in the large diagram only the four nearest octants are shown complete the remainder having the symmetry shown in the smaller diagram. All the octants contain the same tetrahedral arrangement of oxygen ions, the sites being defined by four corners of a smaller cube, which in practice is usually slightly distorted. In the octants corresponding to the unshaded parts of the small diagram, the remaining corners of the smaller cube are occupied by metal ions. In the alternate octants these corners are not occupied; instead there is a site in the centre of the octant. This site being surrounded by a tetrahedral arrangement of oxygen ions, is called a tetrahedral site or A site. A tetrahedral site is shown separately at the top of the diagram. All the black spheres are in tetrahedral sites although this is not obvious where considering only one isolated unit cell. The remaining metal ion sites are surrounded by six oxygen ions in the form of an octahedron. These are referred to as octahedral sites or *B* sites; an isolated octahedral site is shown at the bottom of the diagram.

In the unit cell there are 64 possible tetrahedral sites and 32 possible octahedral sites. Of these only 8 tetrahedral and 16 octahedral sites are occupied in a full unit cell. If in the

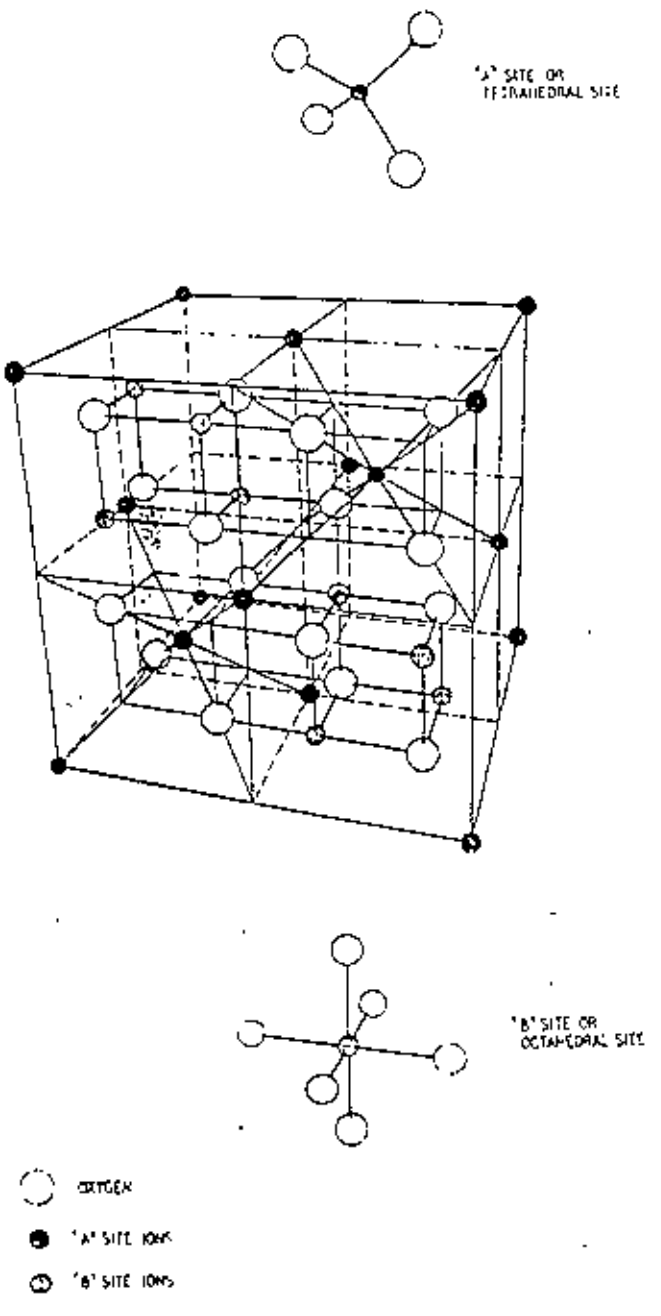

Fig. 4.1 A unit cell of the spinel lattice

preparation the ratio of metal ions to oxygen ions is too small, i.e. there is excess oxygen then some of the metal ion sites may be unoccupied. These sites are then referred to as vacancies. If the ratio is correct, then the unit cell contains 24 metal ions and 32 oxygen ions, i.e. there are 3 metal ions for every 4 oxygen ions. Thus the spinel unit cell may be considered from the chemical point of view to consist of 8 molecules having the formula $MeFe_2O_4$. Of the three metal ions, one is on a tetrahedral site and two are on octahedral sites. If the spinel were 'normal' the divalent *Me* ion would occupy a tetrahedral (*A*) site while the trivalent *Fe* ions would occupy the octahedral *(B)* sites. In an 'inverse' spinel the divalent Me ion occupies one of the B sites while the trivalent Fe ions occupy the other *B* site and the *A* site. In terms of a unit cell:

		Me	Fe_2	O_4
Number of ions	*A site*	– –	8	32
	B site	8	8	

In practice spinel ferrites have an ion distribution some-where between normal and inverse.

The spinel structure consists of a number of interlaced face-centred cubic lattices. The most obvious one in figure 1.1 is that formed by the *A* sites on the cell corners and face centres. The remaining *A* sites (octant centres) form another-face-centred cubic lattice displaced from the first along the cube diagonal.

The positions of the oxygen ions are also defined by a set of interlaced face-centred cubic lattices. Any oxygen ion may be taken as occupying a corner of a face-centred cube having the same dimensions as the unit cell; all other sites in this face-centred cube are also occupied, by oxygen ions. Again, the octahedral (*B*) ions occupy sites on four face-centred cubic lattices. Each of these lattices has the same dimensions as the unit cell and they are displaced from one another along the edges of the smaller tube in the unshaded octants. These interlaced lattices are called sub-lattices and they play an important part in the magnetism of ferrites.

4.2.2 Magnetization

Electrons spin about an axis and by virtue of this spin and their electrostatic charge, exhibit a magnetic moment. Normally, in an ion with an even number of electrons, the spins or moments cancel, and when the number of electrons is odd there will be one uncompensated spin. For the transition metals the number of uncompensated spins is larger, e.g. the trivalent *Fe* ion has a moment equivalent to five uncompensated spins.

When the atoms of these transition metals are combined in metallic crystals, as they are, for example, in parallel alignment over regions within each crystallite. The net number of uncompensated spins will be less than for the isolated ion due to the band character of the electron energies in a metal. The regions in which alignment occurs are called domains and may extend over many thousands of unit cells. The spin orientation is along a direction of minimum energy, i.e. external energy is required to deflect the magnetization from this direction and if the external constraint is removed the magnetization will return to a preferred direction. This directional or anisotropic behavior may arise from a number of factors. Crystal anisotropy is inherent in the lattice structure; the magnetization always preferring the cube diagonal or cube edge. Mechanical strain can cause anisotropy and the shape of the grain boundary will nearly always produce anisotropy. The result is that the magnetization is held to a certain direction, or to one of a number of directions, as if by a spring. The greater the anisotropy the stiffer the spring and the more difficult it is to deflect the magnetization by an external magnetic field, i.e. the lower the permeability.

The parallel spin alignment implies that the material within the domain is magnetically saturated. The magnetization is defined as the magnetic moment per unit volume and is

therefore proportional to the density of magnetic ions and to their magnetic moments. This magnetism arising from parallel alignment is called ferromagnetism.

In a ferrite the metal ions are separated by oxygen ions As a result of this the ions in the *A* sub-lattice (tetrahedral sites) are orientated antiparallel to those in the *B* sublattice (octahedral sites). If these sub-lattices were identical the net magnetization would be zero in spite of the alignment and the ferrite would be classified as anti-ferromagnetic. In the majority of practical ferrites the two sub-lattice are different in number and in the type of ions so that there is a resultant magnetization. Such materials are classified as ferromagnetic. For example, in the foregoing section it was stated that in the general spinel molecule $MeFe_2O_4$ one metal ion occupies an *A* site while two occupy *B* sites; thus in the case of $MnFe_2O_4$ where both metal ions have 5 uncompensated spins the net magnetization is 5 spins per molecule. This compares with a net moment of 2.2 spins per atom in the case of metallic iron. For this reason a ferrite has a much lower saturation magnetization ($\mu_0 M_{sat} \approx 0.5$ *Wb.m*$^{-2}$) than metallic iron (*about 2.0 Wb.m*$^{-2}$). However, in spite of the partial cancellation of the spin moments, ferrites possess sufficient saturation magnetization to make them useful in a wide range of applications.

4.3 Manufacture

4.3.1 Manufacturing processes

The processes used in ferrite manufacture on a industrial scale are similar to those used in the manufacture of other ceramics. The description of these processes given in this chapter is intended mainly for the information of the use. So that the possibilities and limitations of manufacture may be taken into account when a particular ferrite are design or application is being considered. For conventional manufacture of polycrystalline ferrites, a typical flow diagram is shown in figure 4.2. This diagram shows alternative processes, e.g. wet and dry milling and forming and final shapes by pressing or extrusion In fact wet milling is often used in the production of both pressed and extruded parts. Other process variations are possible; some will be mentioned in the more detailed description that follows.

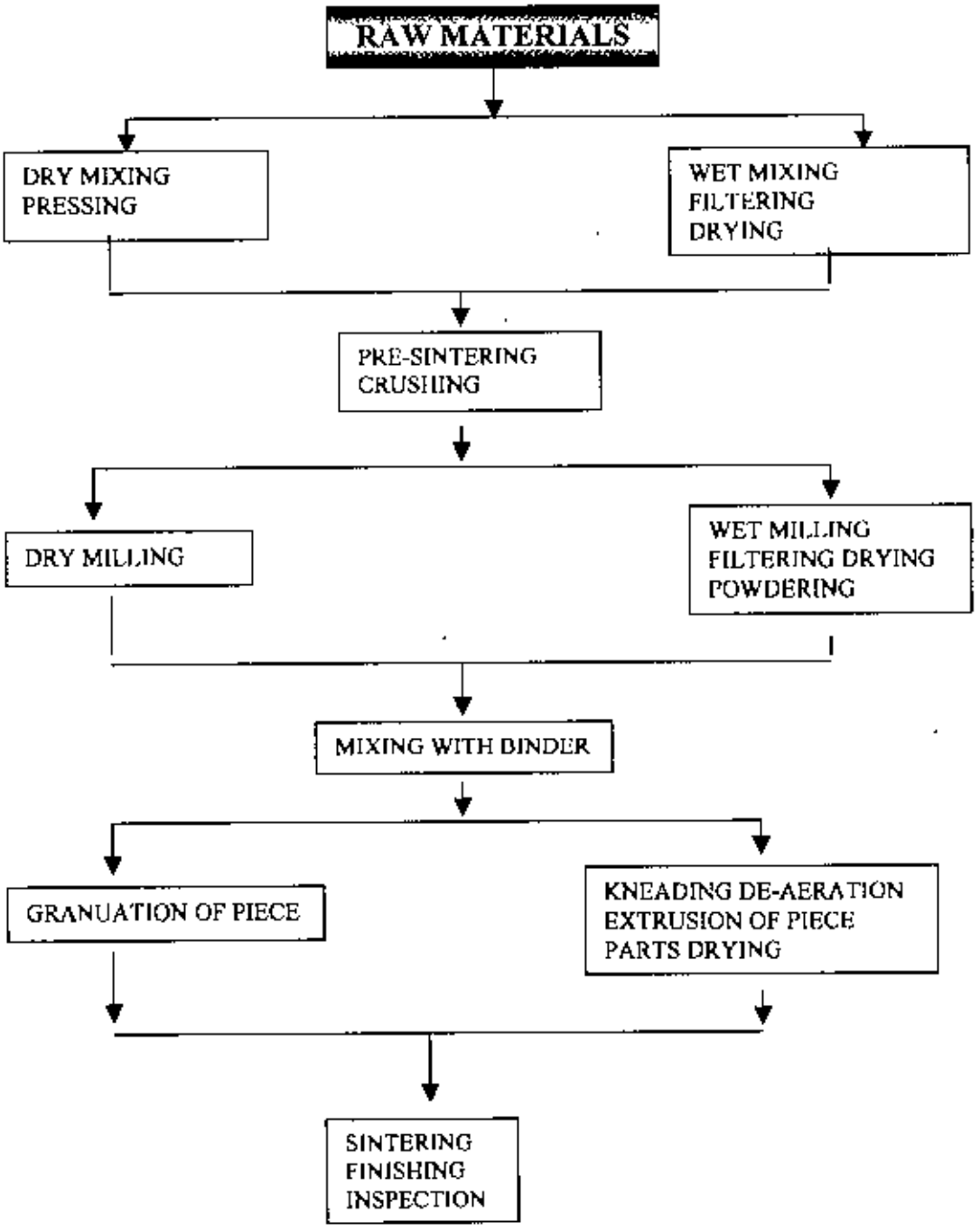

Fig. 4.2: Flow Diagram

4.3.2 Raw materials

The raw materials are normally oxides or carbonates of the constituent metals. Chemical analysis, particle size and price are important characteristics of these starting materials. Because constituents or impurities may have a great influence on the properties of the finished ferrite it is normal to analyze incoming materials in an attempt to ensure that the composition does not deviate significantly from batch to batch. Particle size of the starting material has a profound effect on the behavior of the product during Manufacture [4.10]. The case of mixing, the compressibility, the shrinkage and the reactivity all depend on the particle size so it is normal to keep a check on this parameter to ensure uniformity between batches. Materials of adequate purity and uniformity between batches. Materials of adequate purity and uniformity are usually prohibitively expensive, and successfully large-scale manufacture depends on the skill with which reasonably priced materials may be used to produce constituently ferrites having the required magnetic properties. The constituent raw materials are weighed into batches to give the proportions required for the composition. We have used the wet melling process to make our composition such as $Ni_{0.5-x}Zn_{0.5}Co_xFe_2O_4$ [x = 0.2, 0.3, 0.4] and $Mn_{0.5-x}Zn_{0.5}Co_xFe_2O_4$ [x = 0.2, 0.3, 0.4].

4.3.3 Mixing

The main purpose of this process is to combine the starting materials into a thoroughly homogeneous mixture. If crystallites of uniform composition and properties are subsequently to be formed then constituents must be present in the correct proportions in any microscopic volume of the bulk material. We used wet ball milling method. The constituents are placed in a rotating steel lined drum with steel balls and a medium such as water, steel is used because any iron picked up by the mixture due to wear of lining and balls may be allowed for in the initial composition of the powder. The fluid is mainly

for cooling and mixing purposes. Wet milling usually continues for periods up to about twelve hours. After wet mixing the product is poured of as a starry into a filter press where the water is squeezed out. The resulting blocks are then dried in an oven. In the dry process the powder has to be bossily pressed into blocks ready for pre-sintering. The pressing into blocks makes the product easier to manage in the kilns and improves the thermal conductivity.

4.3.4 Pre-sintering

Pre-sintering or pre-firing is a calcining process in which the temperature of the powder is raised to the region of 1000^0C. Strictly this is not essential to the preparation of ferrites but it is very essential to the preparation of ferrites but it is a very important means of obtaining the necessary degree of control over the properties of the finished product.

Swallow and Jordan [4.11] state that pre-sintering is carried out for the following reasons:

1. It decomposes the carbonates or higher oxides thereby reducing the evolution of gases in the final sintering.
2. It assists in homogenizing the material.
3. It reduces the effects of variations in raw materials.
4. It reduces or controls the shrinkage occurring during the final sintering.

A typical pre-sintering cycle for manganese zinc and nickel zinc ferrites consists of passing the powder down a tunnel kiln in air so that its temperature is raised to a peak of 340-1060^0C in about 8 hours and then allowed to fall until it emerges from the kiln at about 200^0C, about 20 hours after entry. During this process the constituents partially react to form ferrite, i.e. spinel crystals begin to form and are normally allowed to grow to

about 1μ in size. the extent to which spinel is formed depends on the reactivity of the material, the temperature of the kiln and the time for which the material is heated.

4.3.5 Processing of the pre-sintered powder

The pre-sintered powder is milled to reduce it to small, uniformly sized crystallites. This process is carried out in a wet ball mill or a vibrating mill. In either case steel balls are normally used and as previously stated the inevitable wear of the balls may be allowed for in the composition; balls of other materials might cause contamination.

Milling times of up to 12 h are commonly used. After an initial period of rapid breakdown the particle size decreases in proportion to the milling time and then approaches a limiting value. The extent of the milling affects the forming characteristics of the powder, the sintered density and the magnetic properties such as permeability and losses. Since the extent of the milling depends on milling efficiency as well as the milling time it is preferable to mill to a certain particle size rather then a certain time. Particle size may be controlled by measuring the aggregate surface area of the particles in a sample of the powder.

After wet milling, the starry is drawn off and the bulk of the liquid is removed by a pressure filter. The filtered material is then oven-dried and powdered. The dry-milled powder does not, of course, require this treatment.

At this stage it is usual to add the binder and lubricants. The choice of these additives depends on the subsequent granulation process, the method of forming (pressing or extrusion), the required strength of the formed piece-part before firing, and the avoidance of undesirable residues after burning-out during sintering. Commonly used binders are

gum arabic, ammonium alginate, acrylates, polyvinyl alcohol, while waxes and wax emulsions, zinc or ammonium stearate may be used as lubricants to ease powder flow during forming. The quantities involved are quite small; using water as a vehicle these additives are blended with the powder to give the right consistency. Sometimes the lubricant is added later, when the powder has been granulated.

4.3.6 Forming

For the ferrites, the usual forming method is dry pressing by using binders. In its simplest form this process consists of pouring the correct quantity of granulated powder into the die and then closing the die with a prescribed pressure which is usually in the range 1.6 to 16 kg mm^{-2}. We have used three types of die and got three types of shape of the samples. Such as disc (14 mm diameter 2 mm thick), ring [outer dia = 11.07 mm and inner dia = 6.06 mm], and rod [3mm dia and length 45 mm] etc. Figure (4.3) (a) shows the simple pressing of a cylinder and indicates by shading the higher pressure zones caused by friction. If the length l were long enough, the friction alone would be enough to balance the applied force and the powder at the bottom of the die would not be compressed at all. This difficulty may be somewhat alleviated by compressing the powder from both ends as in figure (b). In practice it is usual for the die to move in a vertical line during pressing, the movements of die and punches being so related that the most uniform pressed density is obtained. Even so, shapes having l/d ratios of greater than about 5 are difficult to press successfully.

Inhomogeneons pressed density leads to inhomogeneous magnetic properties and so degrades the product. It also leads to non-uniform shrinkage during the sintering and this causes shape distortion as shown in exaggerated form in figure (c). In more complicated

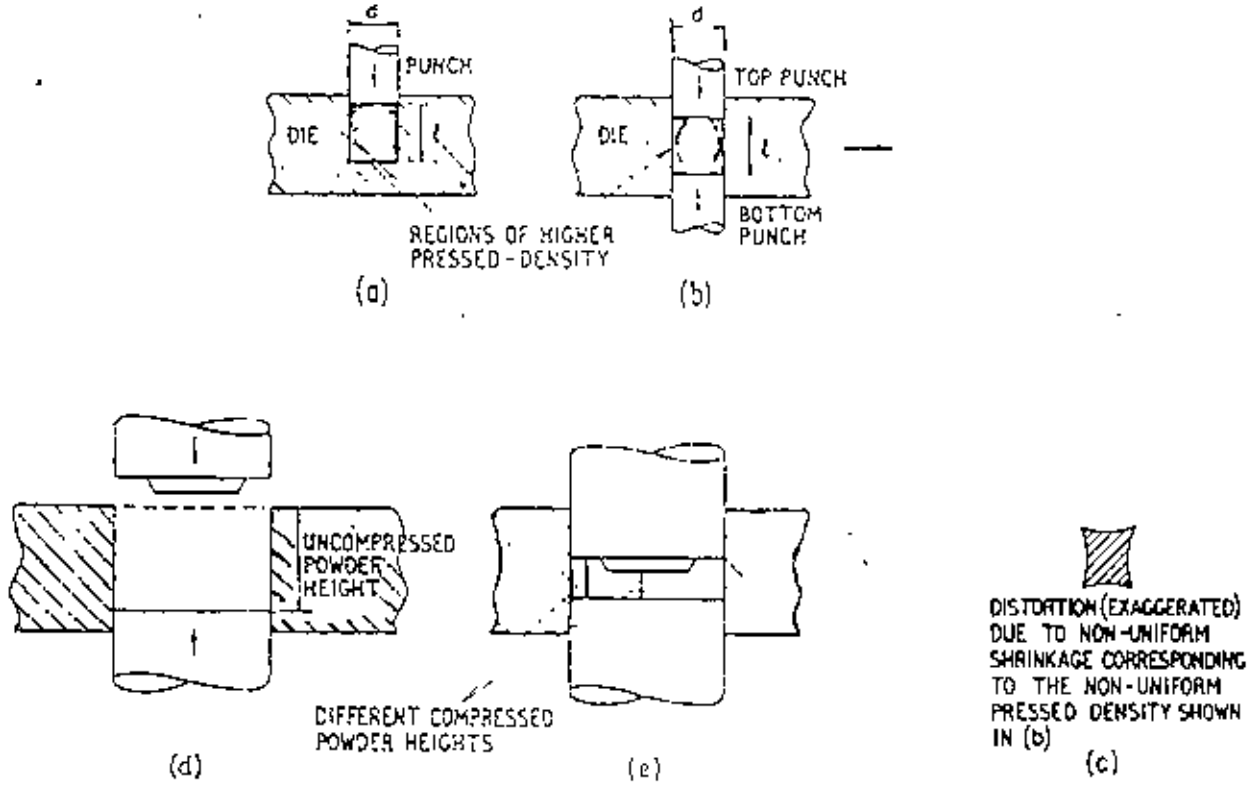

Fig. 4.3 Forming method of samples

shapes non-uniform pressed density may result from some zones being compressed more than others, see figures (d) and (e).

4.3.7 Sintering

In the compacted form the partially reacted particles press against each other over part of their surface, the remaining surface forming the boundaries of the interstitial voids or pores. At temperatures in the region of 1000 c and above, the free surface containing the voids decrease, the particles grow together to form crystallites and the density rises. During this process the linear dimensions of the piece part shrink between 10% and 25% depending on the powder and the pressing technology and this must be allowed for the design of the forming tool. The grain growth and the elimination or the persistence of pores both have profound effects on the properties of the sintered ferrites[4.12, 4.13]. Typical crystallite sizes range from about 5 to 40μ.

The properties are of course, also affected by changes occurring within the crystallite structure. These changes are influenced not only by the temperature but also by the atmosphere in which the sintering takes place in particular the partial pressure of the oxygen in the atomosphere.

A mixed ferrite in a quaternary system such as *Mn-Zn-Fe-O* can exist in a wide variety of compositions within the limitations of the spinel structure. Even when the proportion of the three metals is fixed during powder preparation the valency states and the phase depend on the amount of oxygen in the structure and this will depend on the oxygen equilibrium between the structure and the surrounding atmosphere. If, for instance, the partial pressure of oxygen in the atmosphere is very small, any excess iron the

composition would be present as ferrous ions and would take its place with the other divalent ions, e.g. *Mn* and *Zn*. A small proportion of ferrous ions together with manganese ions tends to increase the permeability and reduce the losses, but the co-existence of trivalent and divalent ions of the same element lowers the electrical resistivity.

4.3.8 Inspection

After sintering we have got ferrite samples in various shapes. These samples are checked by using X-ray diffraction which is shown in figure (4.4). From the result of X-ray, these ferrites samples have been produced correctly and they are face-centered cubic lattice. Beside this the mechanical dimensions are checked by conventional method. The magnetic properties pose greater problems. For a typical ferrite core it is necessary to control about seven magnetic parameters and some of these present appreciable measuring difficulty, e.g. the measurement of very low magnetic losses, temperature co-efficient of permeability, etc.

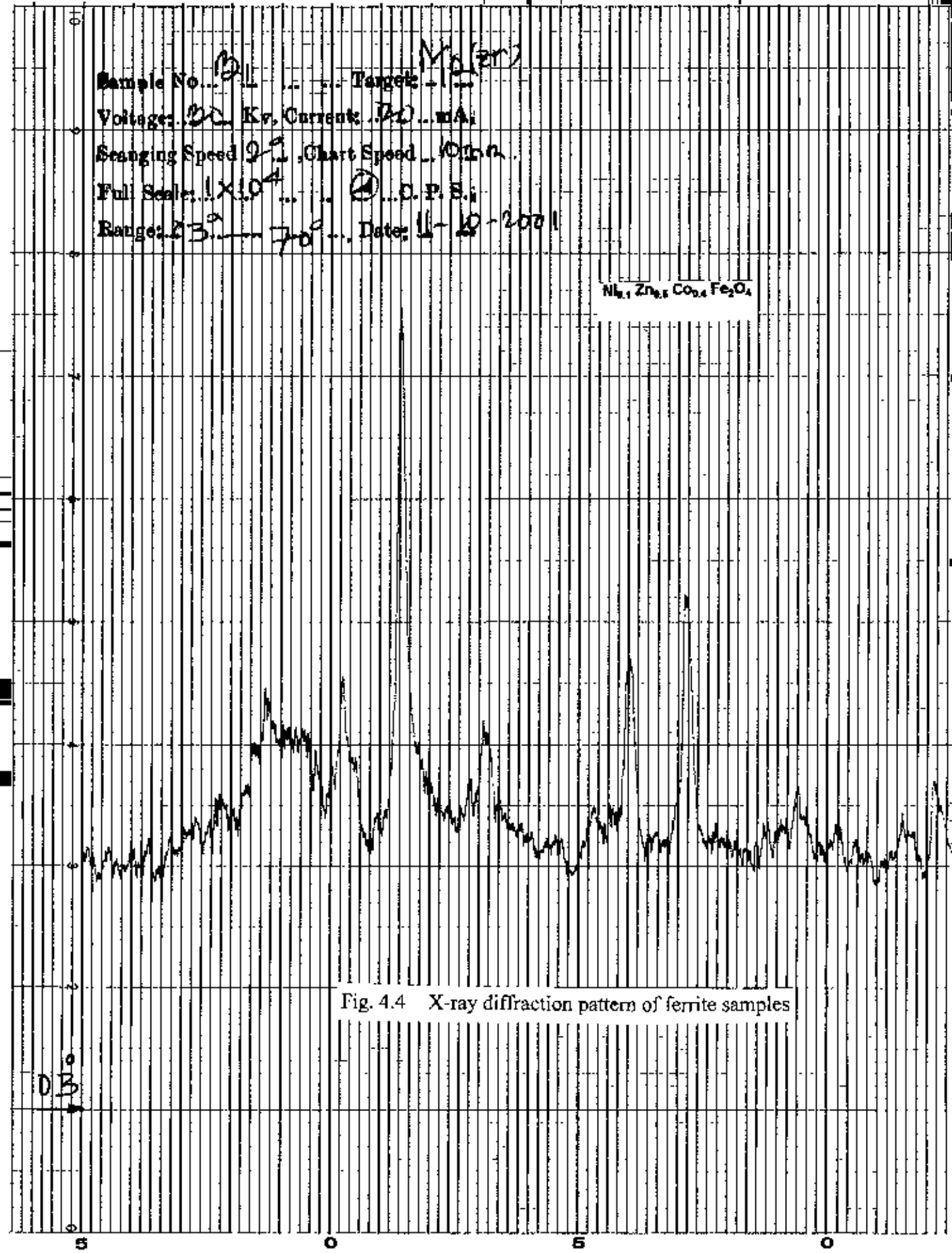

Fig. 4.4 X-ray diffraction pattern of ferrite samples

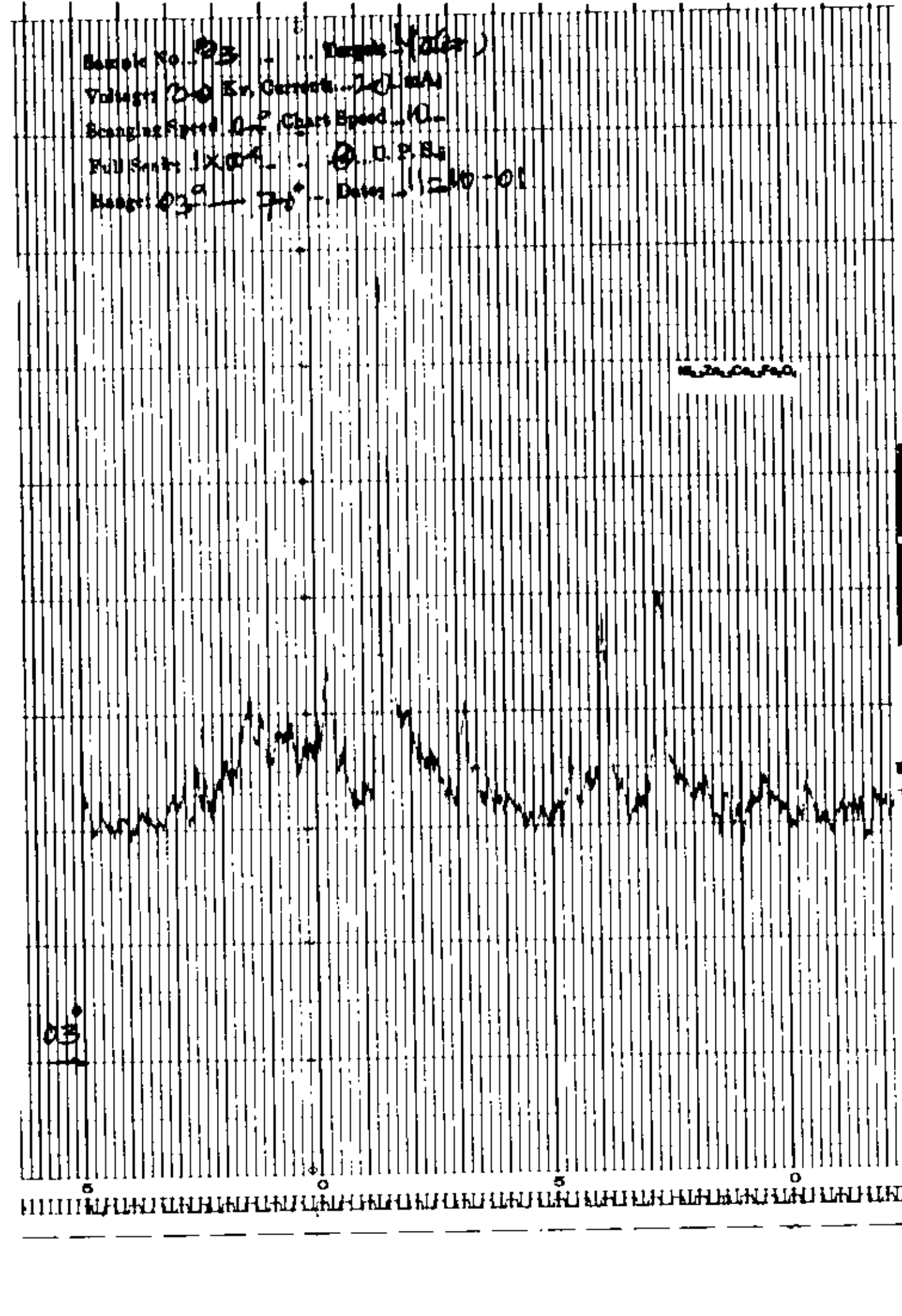

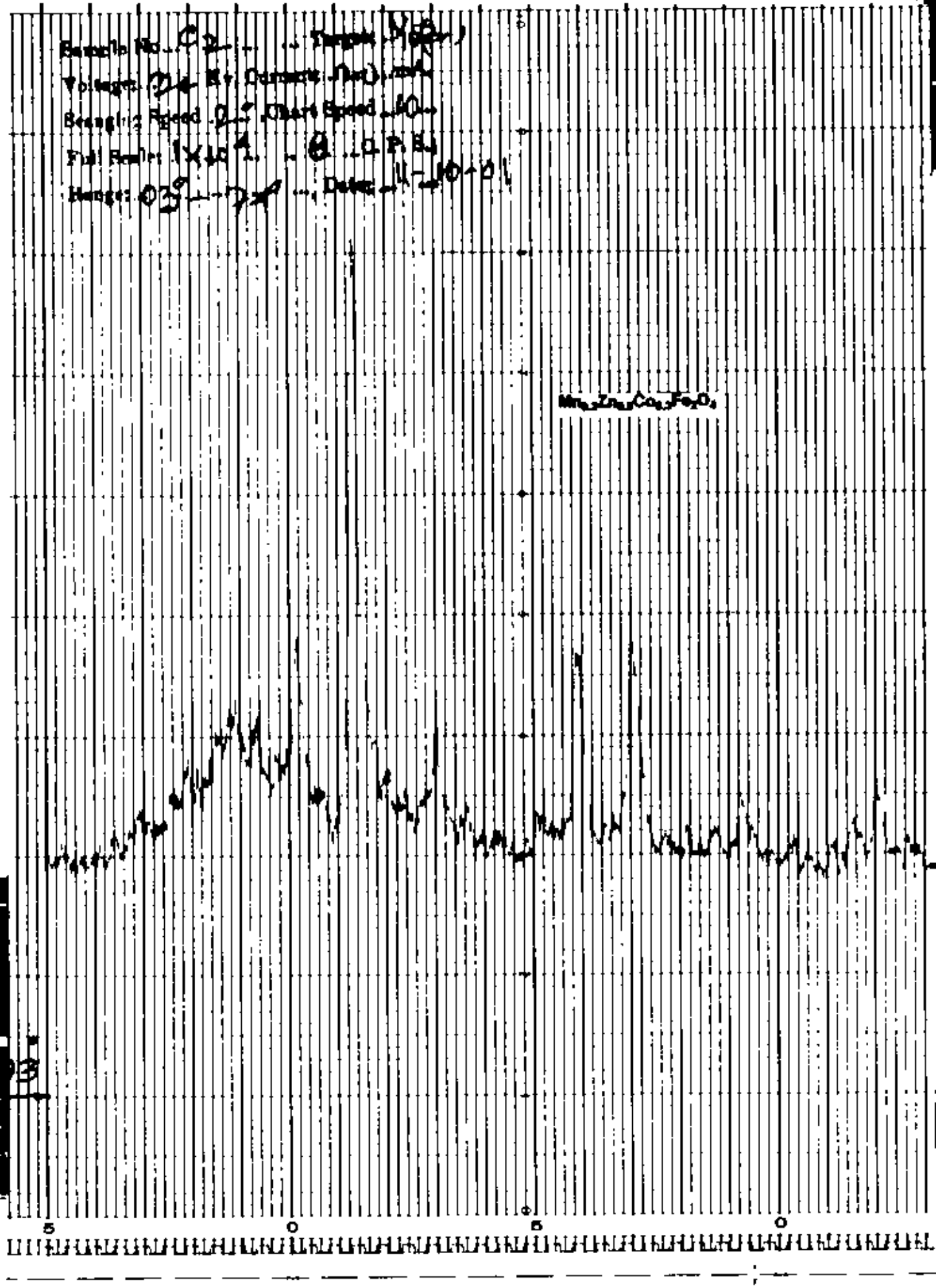
$Mn_{0.5}Zn_{0.5}Co_{0.5}Fe_2O_4$
5
0
5
0

CHAPTER - V

Measurement-Magnetostriction and Thermal Expansion

5.1 Magnetostriction Measurement Technique
5.2 Strain Measurements using Strain Gage
5.3 Gage Factor
5.4 Calibration curves for Magnet
5.5 Bridge Current Sensitivity and Calibration
5.6 Calibration Curve for Angle Correction
5.7 The Specimen Holder
5.8 Specimen mounting
5.9 Temperature Measurement and Control
5.10 The Magnet
5.11 The Gage Cementing

CHAPTER V

MEASUREMENTS- MAGNETOSTRICTION AND THERMAL EXPANSION

5.1 Magnetostriction Measurement Technique

This technique, since the time of its introduction by Goldman [5.1] has gradually replaced almost entirely all other methods of magnetostriction measurement. The reason for this success, as also the problems associated with this method and some of the improvement in the use of this technique as developed by M. A. Asgar[5.2] are as follows

Magnetostriction measnrements are set with a large number of problems. Strain developments in a magnetic specimen, when magnetized. This small strain is developed both on the direction of magnetization and its magnitude. Also the state of zero average external magnetization may not correspond to the zero magnetic strain, because the demagnetized multidomain state is neither unique nor well defined.

In the displacement method Nagaoka [5.3] combined optical and mechanical methods. Here the specimen, by the displacement of its free end, the other end being fixed, rotates a spindle to which a mirror is attached. A beam of light reflected off this mirror forms optical lever.

The difficulty with this method is that one has to use a big specimen to get sufficient sensitivity. Again it is difficult to magnetize a big specimen in different direction using rotating field, maintained at uniform field and steady temperature. Again this method cannot provide the strain difference of two well-defined magnetic states one has to assume equal distribution of the domains in all the easy direction of magnetization in the demagnetized state, which may not be true.

The x-ray diffraction technique which was first used by Rooksby and Willis [5.4] to determine spontaneous magnetostriction, measures the distortion of crystal axes by determining (c/a - 1) directly from the magnitude of the splitting of x-ray reflection spots from different crystal planes.

However, x-ray method besides being less sensitive is difficult to use with different direction of magnetization. In using strain gauge technique one can get over many of this difficulties. The gauges can be used on a very small disk shaped specimen cut in a definite crystallographic plane and the gauge can be bonded in a precisely determined direction.

The strain gauge works on the principle that when a fine wire in the form of a grid or a thin foil, and embedded in a paper or epoxy film is bonded firmly on a specimen and shows a change in resistance proportional to the strain.

We can write this relation as

$$\frac{dR}{R}=G\frac{dl}{L} \qquad 5.1$$

where $\frac{dR}{R}$ is the fractional change in resistance, G is the gauge factor and $\frac{dl}{L}$ is the strain along the gauge direction.

The magnetic strain in the crystal is determined from the change in resistance of the gauge fixed on the specimen in relation to the resistance of another dummy gauge bonded on a reference specimen using a resistance bridge in the out of balance condition.

The mechanism of resistance change of the gauge wire under strain can thus be quite complex. Moreover, the gauge may not follow the strain of the material on which it is bonded. Thus there is to be affected by bonding factor. In addition one has to consider the thermally induced resistance change, when the dummy and active gauge are at different

temperatures. The most important difficulty with the use of strain gauges in dummy gauge on a suitably chosen nonmagnetic material which have the same thermal and thermoelastic properties as the magnetic material. This ensures that the dummy and the temperature except for the magnetic strain.

5.2 Strain Measurements Using Strain Gauge

In 1947 Goldman was the first to measure magnetostriction by the use of strain gauge a folded metal wire, which can have a resistance of the order of 100 ohms. The strain gauge technique is based on the fact that any strain characteristic of the specimen on which the gauge is fixed is transmitted faithfully to the electrically sensitive zone of the gauge and observed as a resistance changes which can be measured with the help of a whetstone bridge. When the temperature of the specimen is changed there is a further contribution to the resistance change due to thermal expansion of the gauge wires, the gauge matrix, the bonding glue, specimen and the resistivity change and the change in gange factor of the gauge material. Similar strain gauge known as dummy gauge is in the other arm of Whetstone Bridge to compensate as far as possible for temperature influence.

The measurement can be carried out with direct current or low frequency alternating current (f<100 c/s) since the magnetic material to which the current carrying wires are fixed can give rise to an inductive effect which changes during magnetization. This method is also very sensitive, being capable of measuring strains up to 10^{-8}. The minimum dimension of strain gauges are approximately 2 mm. Additional error that can occur in this measurements is magnetoresistance of the wire. At room temperature this is not greater than 10^{-7}.

When more than one strain gauge (active and dummy) is used in a whetstone bridge circuit. This effect is approximately eliminated if care is taken to ensure that all the strain gauges are in the same magnetic field.

5.3 Gauge Factor

It is observed experimentally that the resistance of a thin wire varies proportionally to the strain to which it is subjected, provided the temperature is constant and the applied strain is small. This provides the definition of gauge factor of the wire as the fractional change in resistance per unit strain

$$\text{i.e.} \qquad G=\frac{\Delta R/R}{\Delta l/l} \qquad 5.2$$

5.4 Calibration Curves for Magnet

The electro-magnet that used for the measurement of magnetostriction calibrated with electronic fluxmeter to an accuracy of about ±1% A conventional calibration of current I vs field strength H is shown in figure 5.1.

5.5 Bridge Current Sensitivity and Calibration

The current used for measurement of the resistance changes in the gauges was a D.C. Whetstones Bridge figure 5.2. It included a reversing switch (s) to ascertain to what extent thermal E.M.F.'s into the circuit were effecting the balance conditions of the bridge. The nano-voltmeter used was a Model 140 of high sensitivity and a period of 2.5 seconds.

This low periodic time of the instrument enabled quick recording of out-of-balance deflections thus minimizing errors due to drift and fluctuations from thermal E.M.F.'s in

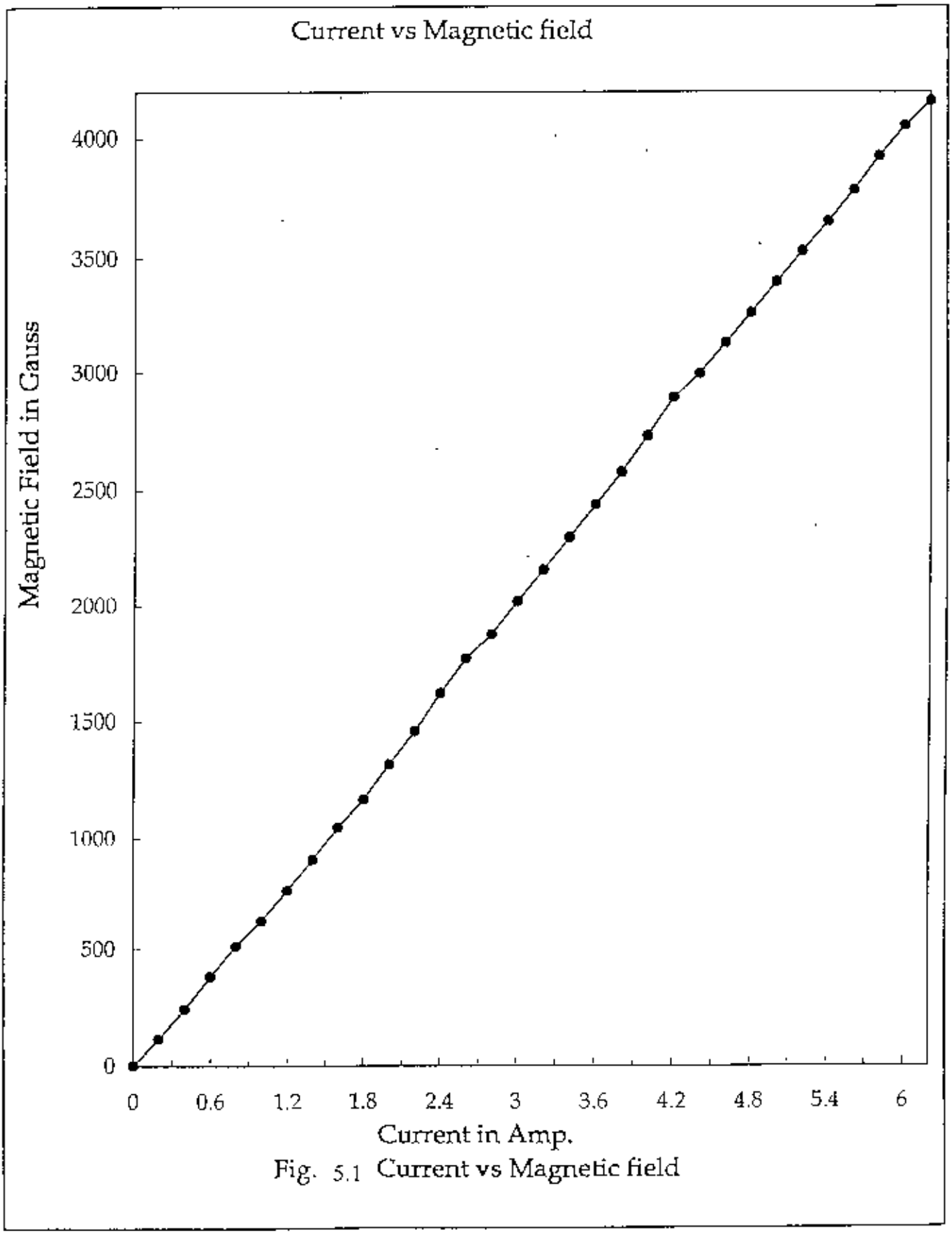

Fig. 5.1 Current vs Magnetic field

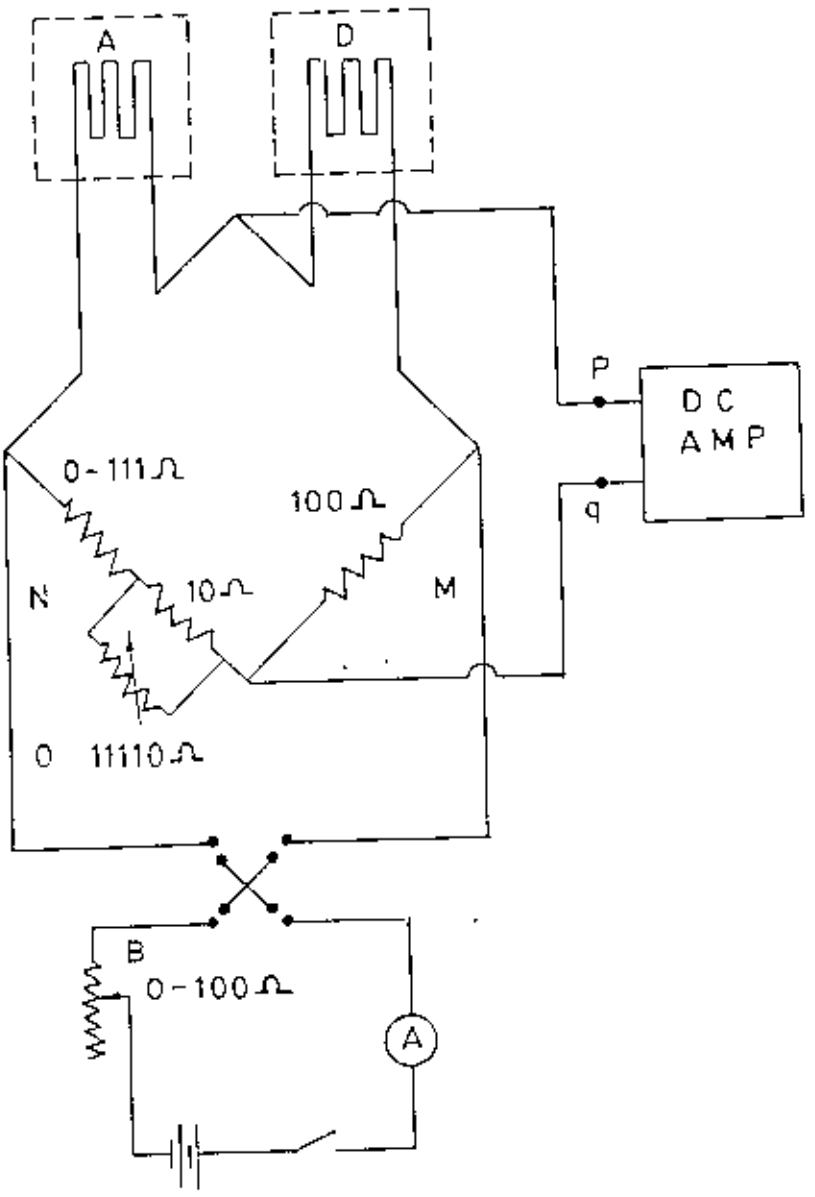

Fig.: 5.2 D.C. Bridge

the circuit. The bridge sensitivity changed linearly with bridge current figure 5.3 and figure 5.4. Bridge current was restricted to a maximum of 5.5 mA to prevent overheating in the gauge elements.

The components of the bridge are shown in figure 5.2 where A represent the active strain gauge in contact with the specimen and D represent the dummy gauge in the same environment as the active gauge. Any thermal fluctuations which occurred in gauge A also accurate in gauge D and since these are in opposing arms of the bridge, the net effect of the fluctuations should be zero.

Work on the bridge arrangement is to continue and it is hoped to amplify small D.C. output voltages from the bridge when measuring very small strains to record the nano-voltmeter scale deflection. Also slow steady thermal drifts would be recorded and allowance made for these in the calculation of results.

5.6 Calibration Curve for Angle Correction

In the polycrystal ferrites the magnetic domains of the different microcrystallites having random orientations make different angles with each other in the demagnetized state. When the magnetic field is applied the magnetic domain wall movement starts. In this way we have to find out the perpendicular and parallel position of the magnet. From this position of the magnet we get maximum and minimum position of magnetostriction. Figure 5.5 has shown the angle vs magnetostriction curve.

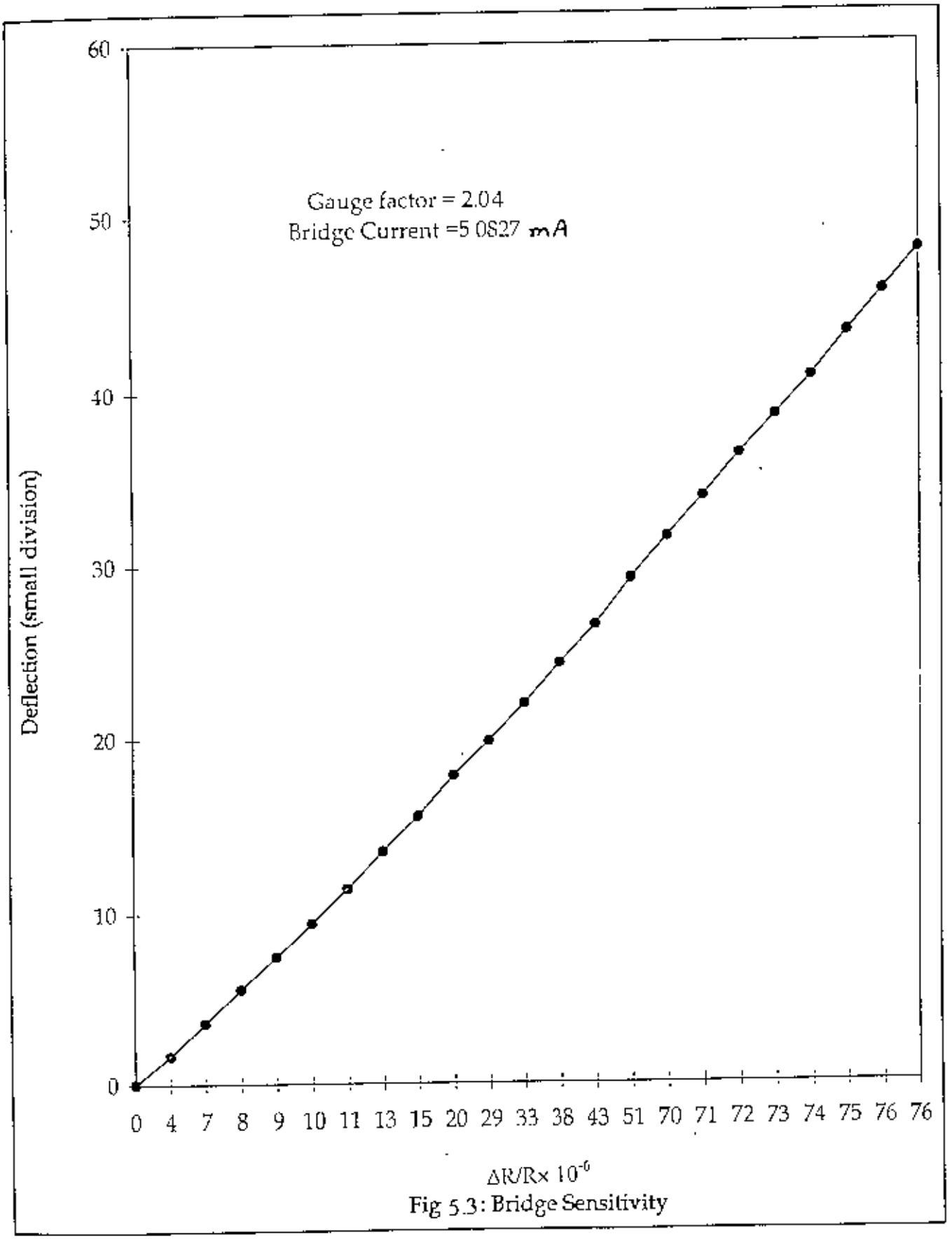

Fig 5.3: Bridge Sensitivity

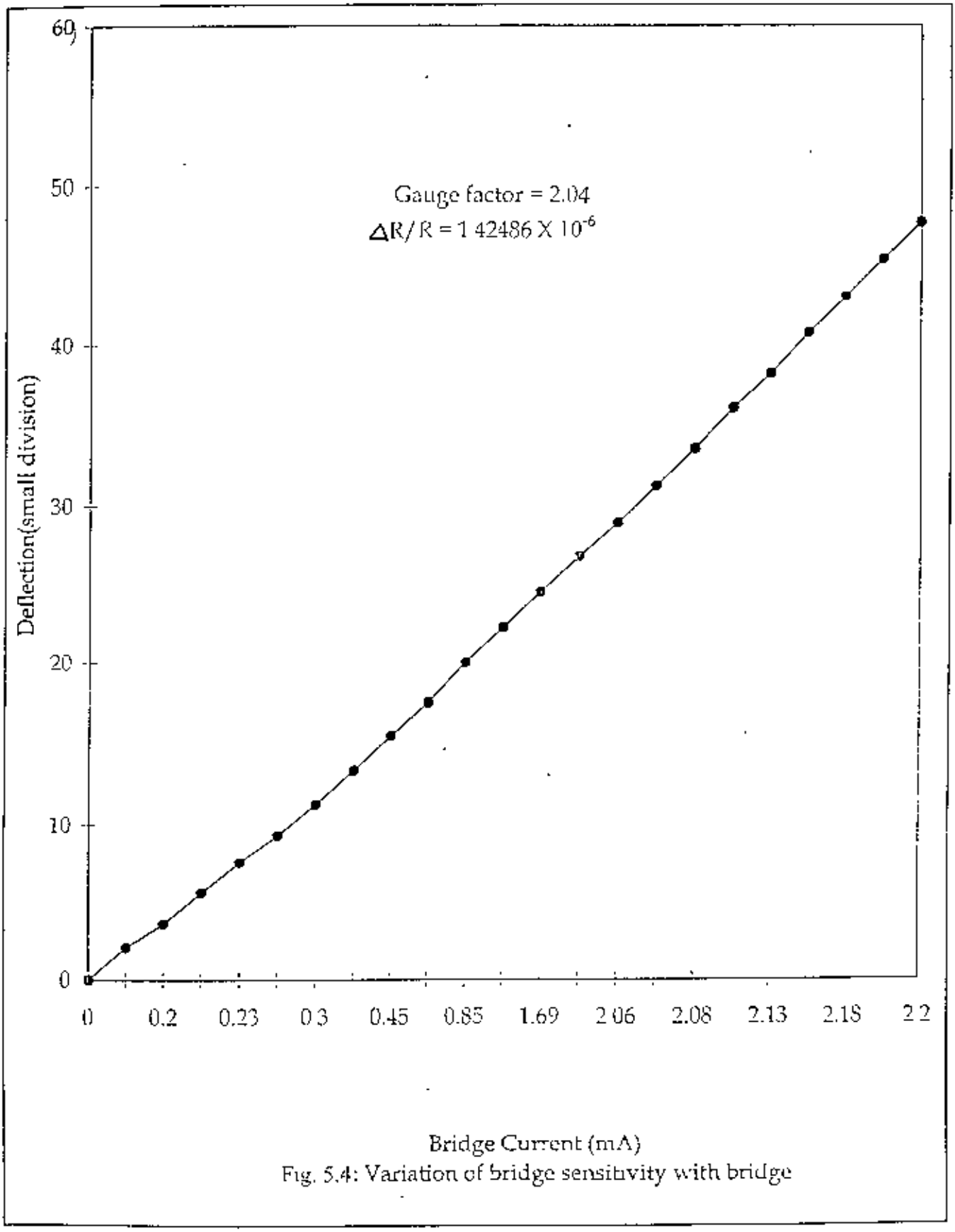

Fig. 5.4: Variation of bridge sensitivity with bridge

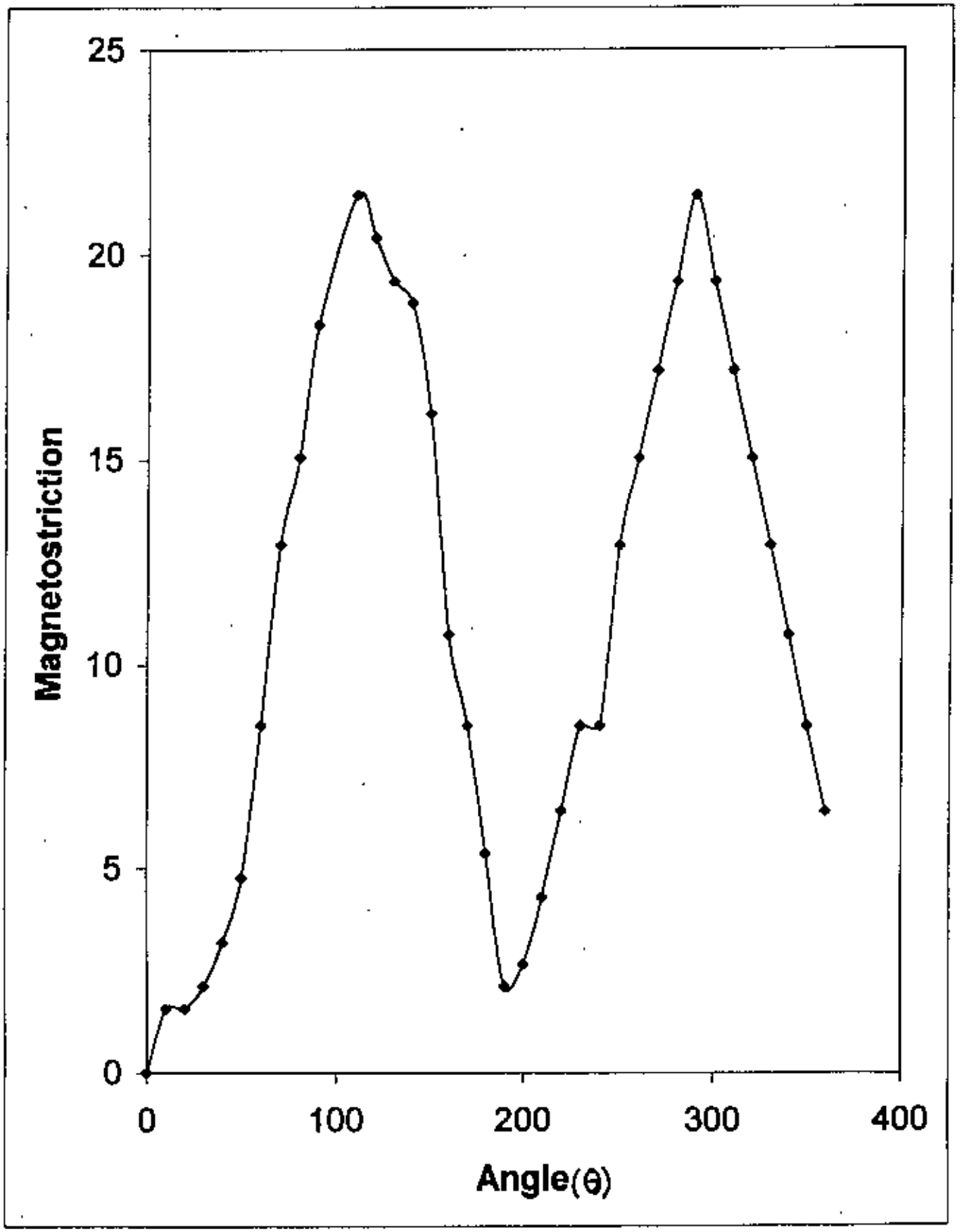

Fig. 5.5 Angle vs Magnetostriction Curve

5.7 The Specimen Holder

It is very important to keep the temperature of the specimen and the dummy identical. Since both are subject to the heating effect of the gauges, it is necessary either to make the size of the samples and dummy large or to contain them in an enclosure of large heat capacity. The latter method is naturally more convenient. A cylindrical shaped enclosure of copper served the purpose and is shown in figure 5.6. The central portion of the hollow cylinder is provided with a platform for the dummy and the specimen to sit on opposite sides. A metallic window was cut which can be closed after the specimens are oriented and the specimens are separated from the metallic platform by the insulating cork.

5.8 Specimen Mounting

To mount a specimen, particularly a ferrimagnetic crystal two opposing factors have to be considered. The crystal must not be mechanically constrained by the specimen holder so that the spontaneous distortions of the crystal due to temperature change or magnetic field can faithfully be transmitted to the strain gauge. Especially, when the crystal is classifically soft but highly magnetic, the mechanical constraint may even cause distortion of the symmetry of the crystal. From this consideration therefore, the mounting has to be flexible. On the other hand, to avoid any rotation of the specimen due to the torque produced by the magnetic anisotropy, the crystal must be held sufficiently rigidly.

The best compromise is made by using a thin cork spacer between the specimen and the base of the specimen holder. The specimen is glued to the cork by durofix and the cork

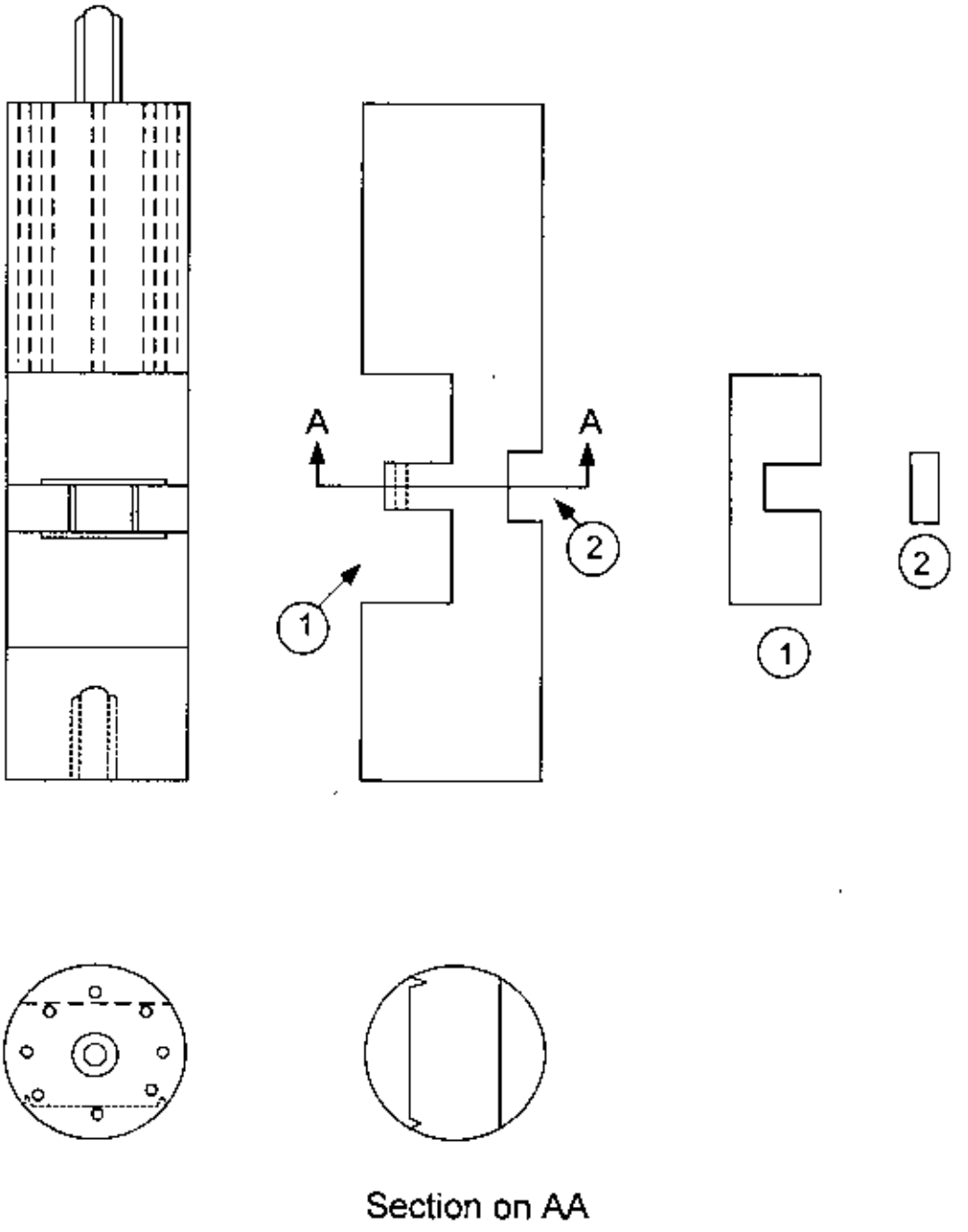

Fig. 5.6: Specimen Holder

in turn to the specimen holder. The mosaic pattern of the cork spacer allows the specimen to expand or contract quite freely but constrains it from rotation due to body forces. Down to liquid helium temperature the arrangement is found to work successfully, comparison of the thermal expansion of a Ferrite specimen when fixed to a cork spacer and when free showed the constraint due to the above mentioned arrangement does not affect the result.

5.9 Temperature Measurement and Control

The whole temperature range from liquid N_2 to room temperature was conveniently measured by means of copper- Tungsten thermocouple made by us. The hand made thermocouple was checked by compared with the standard e.m.f. vs temperature which is shown in figure 5.7. In our experiment temperature is very essential to measure the thermal expansion of the ferrite samples.

5.10 The Magnet

An Newport Electromagnet type F was used for the production of magnetic field. When the maximum current of 100 amp D.C. was used with conical pole tips and a gap of 1.25" the field produced at the centre of the pole pieces was 25 koe.

The magnet could be rotated about a vertical axis through the centre of the pole gaps and could be locked in any position. The angular position of the magnet could be read to one tenth of a degree with the help of the vernier scale fixed at the base. The field versus current curve for the magnet for the pole gap used, was calibrated using a Newport Hall probe magnetometer type H with an active element and is shown in figure 5.8. A very small hysteresis effect was observed for increasing and decreasing currents. Using button control the could be increased or decreased continuously to within 50 mA.

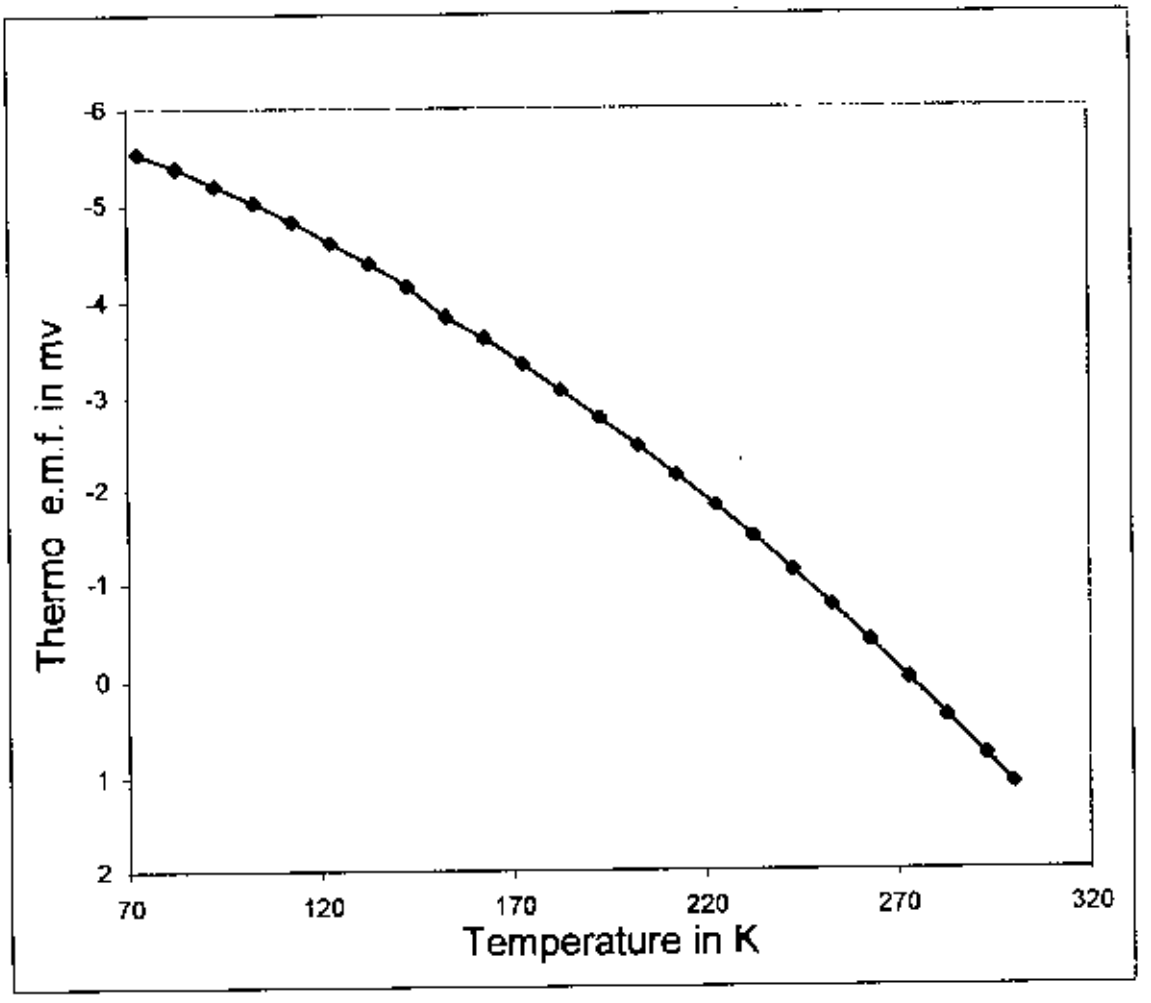

Fig : 5.7 Temparature vs Thermo e.m.f.

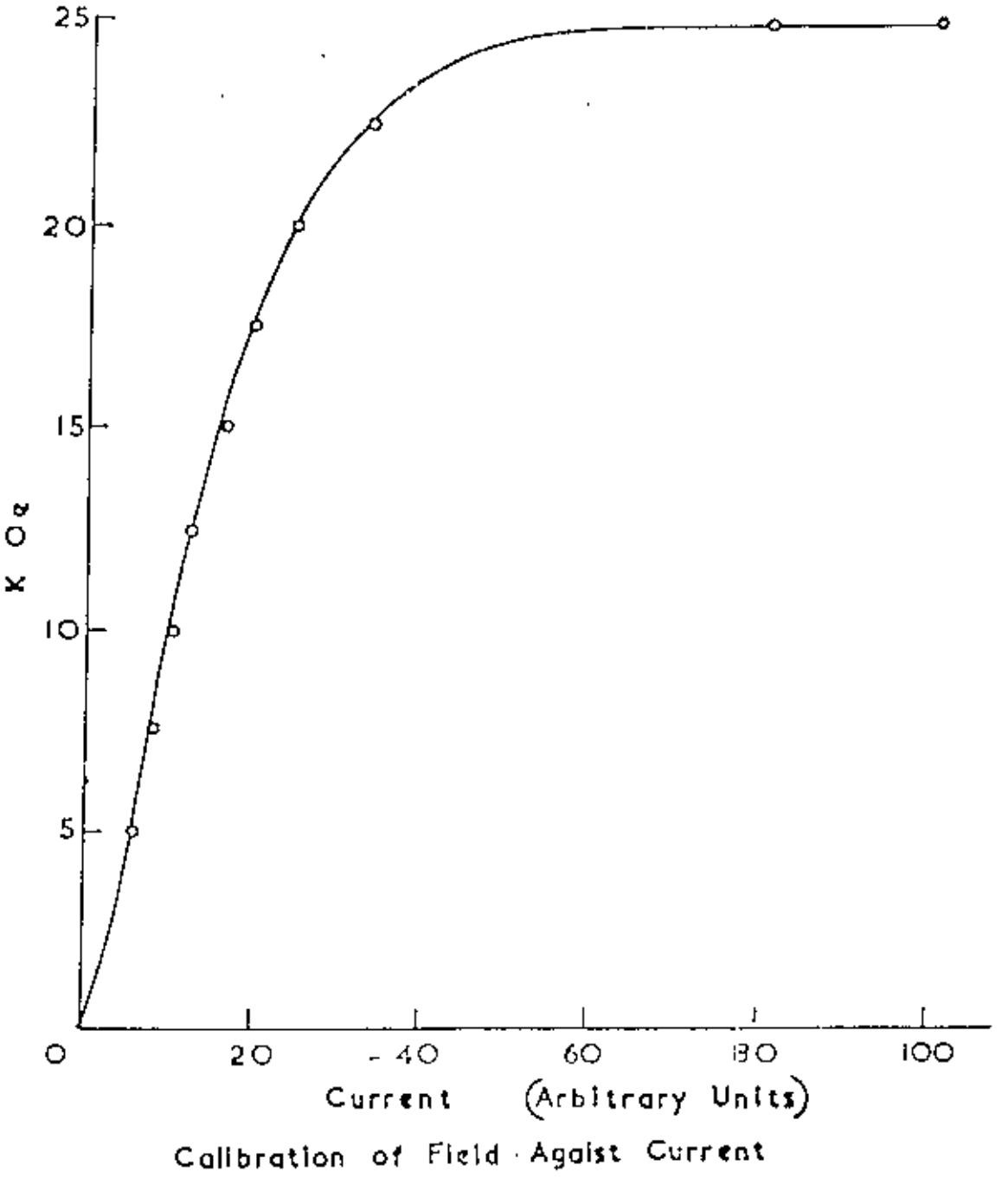

Fig 5.8 Calibration of Field Against Current

5.11 The Gauge Cementing

In order to have perfect gauge bondage between the gauge and the surface of the specimen it is necessary to have specimen surfaces.

Using a special paper glued on both sides the specimen was held fixed with its scratch mark indicating the crystallographic direction, along which the gauge was to be fixed, parallel to the cross wire of the microscope.

A thin coat of adhesive MB-600 was applied to the gauge surfaces and the gauge area of the specimen. The adhesive was allowed to dry for five minutes and the then the gauge was placed on the specimen and with the help of the attached tapes was held fixed parallel to the cross wire.

The gauge was covered with a very thin sheet of Teflon on which the adhesive did not work. A heavy pressure was given on the gauge by the weight. The adhesive was cured for 24 hours at room temperature. The sellotape was removed and the gauge position was checked under the microscope.

CHAPTER - VI

Results and Discussions

6.1 Magnetostriction

6.2 Thermal Expansion

Chapter VI

Results and Discussions

6.1 Magnetostriction

Magnetostriction of the NiZn and MnZn with Co substituted ferrites of new compositions $Ni_{0.5-x}Zn_{0.5}Co_xFe_2O_4$ and $Mn_{0.5-x}Zn_{0.5}Co_xFe_2O_4$ [x = 0.2, 0.3, 0.4] has been measured using strain gauge technique. A random orientation of the magnetic domain have been considered as in the case of polycrystalline materials and the magnetostriction constant $\frac{\Delta l}{l}$ have been measured for different samples using the relation

$$\frac{\Delta l}{l} = \frac{3}{2}\lambda(\cos^2\theta - 1) \qquad 6.1$$

as explained in chapter V.

The most important task is to magnetize the specimen along the direction of the gauge fixed on the specimen and then to rotate the magnetization vector perpendicular to this direction so as to find the difference between the corresponding strains produced in the specimen. We then set from equation (6.1).

$$\left(\frac{\Delta l}{l}\right)_{//} = \left(\frac{\Delta l}{l}\right)_{\perp} = \frac{3}{2}\lambda_{s}(\cos^2 90 - 1) - \frac{3}{2}\lambda_{s}(\cos^2 0 - 1) = \frac{3}{2}\lambda_{s} \qquad 6.2$$

In order to find the exact direction of the strain-measuring gauge, which was carefully bonded on the specimen with respect to direction of magnetization, magnetostriction as a function of the position of the field was measured. The direction of the field was initially obtained arbitrarily with respect to the circular scale at the base of the rotating magnet. From the graph of strains VS field directions as shown in figure 5.5 the exact direction of the gauge related to the field was determined. This was done by using the principle based on equation (6.2) where we find that the maximum differential change in strain

occurs when the magnetization vector is rotated by 90^0 from the position which is parallel to the gage direction to the direction which is perpendicular to it. The field was initially applied parallel to the gauge direction approximately and the maximum differential change was found out by trails.

It is assumed that for sufficiently high field the direction of the field also corresponds to the direction of the saturation magnetization. Figure 6.1 shows the magnetostriction of $Ni_{0.1}Zn_{0.5}Co_{0.4}Fe_2O_4$ as a function of magnetic field. The saturation field is found to be 2.02 k Gauss. This field appears to be large enough for the soft magnetic material. This applied field is also much larger than the effective internal field due to demagnetizing effect, which is necessary condition for saturation magnetization. In order to find the saturation magnetization we only need to measure the strain due to saturation magnetization along the length of the gauge by magnetizing the specimen to saturation value of 21, in the direction perpendicular to the gauge and then in the direction parallel to the gauge. By subtracting the former from later we obtain the saturation magnetostriction constant using the equation (6.2). Each measurement was taken three times with practically no deviations. We varied the field direction and field strength, from their values as shown in figure 6.1. The saturation field was found to be 2.02 K. Gauss. After saturation was reached at 2.02 the field was increased in steps upto 4.16 K. Gauss. No change in magnetostriction value was observed with increasing field. In this way we got saturation magnetostriction of $Ni_{0.2}Zn_{0.5}Co_{0.3}Fe_2O_4$ and $Ni_{0.3}Zn_{0.5}Co_{0.2}Fe_2O_4$, which were 19.80 and 18.44 respectively. The results are summarized in figure 6.2.

From the result we see that of Ni concentration there is decrease in magnetostriction. But the saturation field was more all less same. On the other hand when we measured saturation magnetostriction of $Mn_{0.1}Zn_{0.5}Co_{0.4}Fe_2O_4$ and $Mn_{0.2}Zn_{0.5}Co_{0.3}Fe_2O_4$, which were shown in figure 6.3. We got the saturation magnetostriction 15.20 and 18.90 respectively where the saturation field was 1.875 K. Gauss. Here we see that the increasing rate of Mn concentration is an increase in the value of saturation magnetostriction.

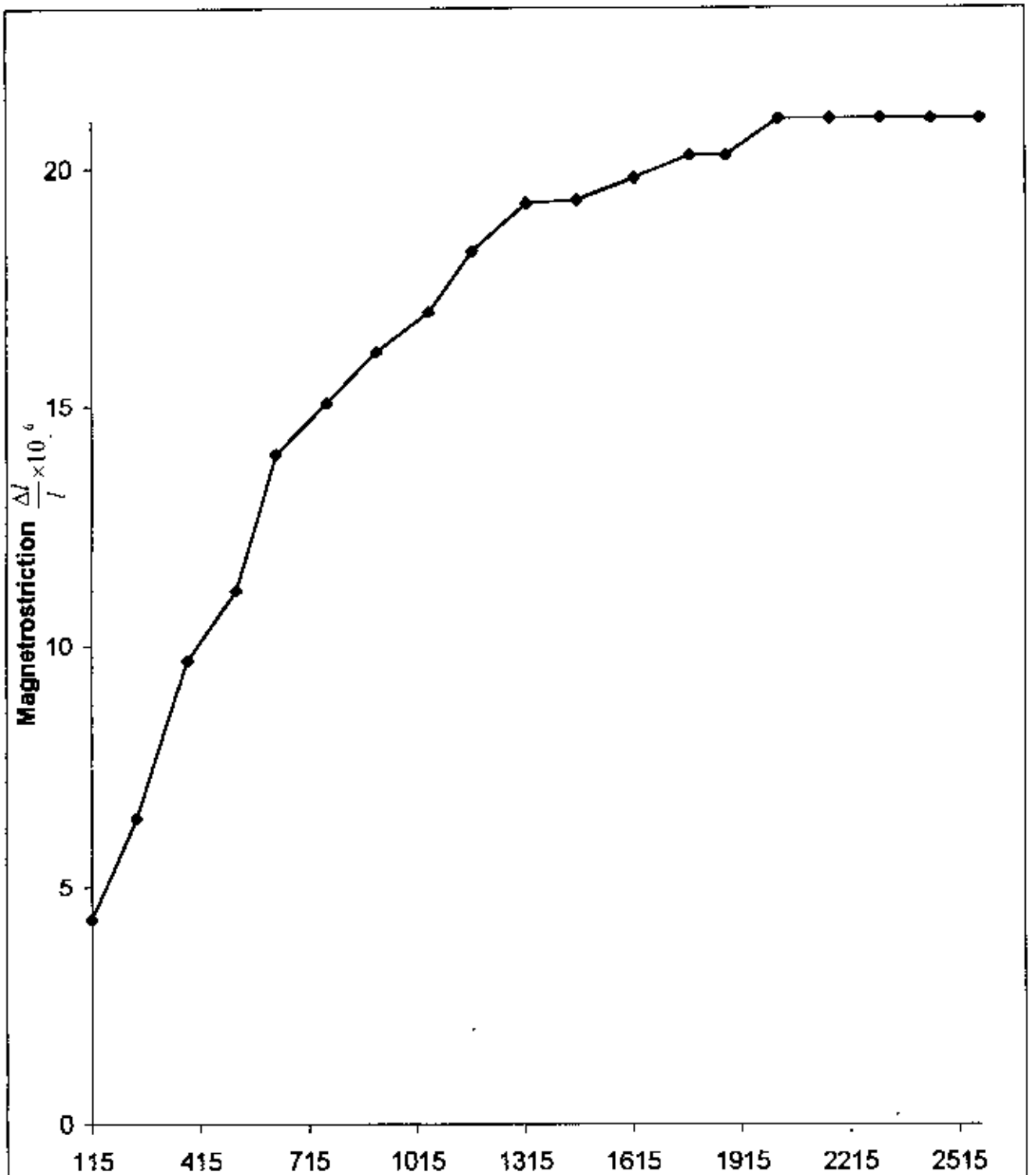

Fig. 6.1: Magnetostriction of $Ni_{0.1}$ $Zn_{0.6}$ $Co_{0.4}$ Fe_2O_4 as a function of Magnetic Field

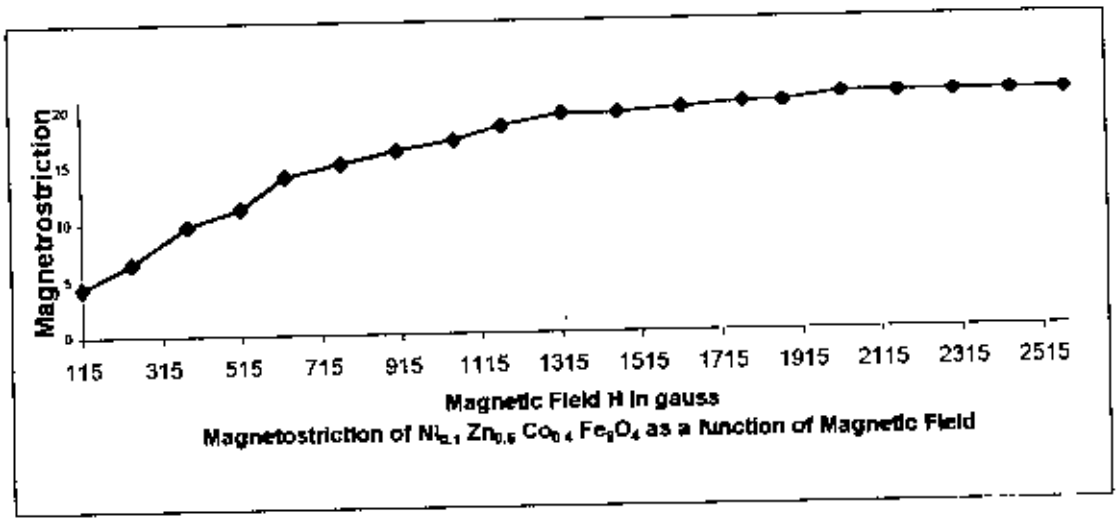

Magnetostriction of $Ni_{0.1}Zn_{0.6}Co_{0.4}Fe_2O_4$ as a function of Magnetic Field

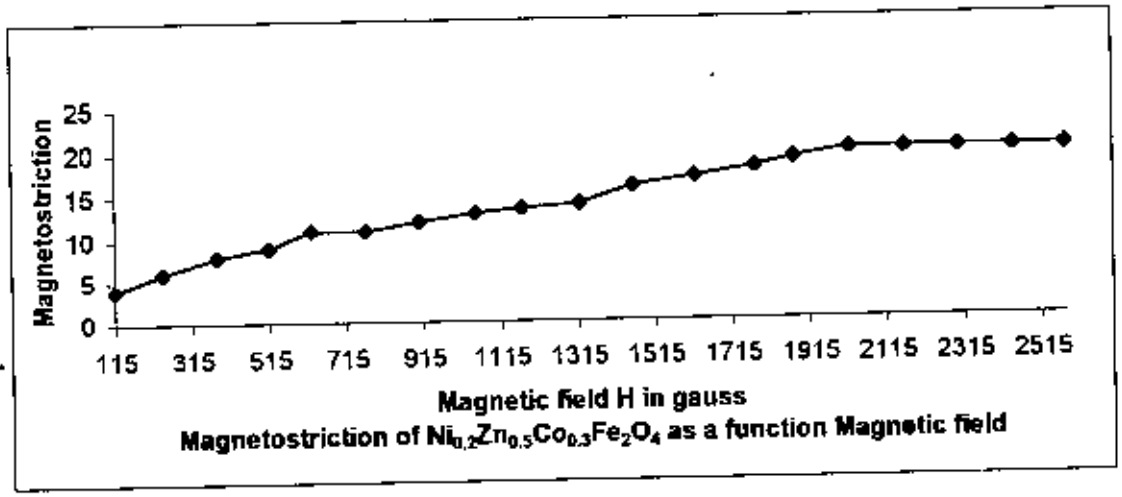

Magnetostriction of $Ni_{0.2}Zn_{0.5}Co_{0.3}Fe_2O_4$ as a function Magnetic field

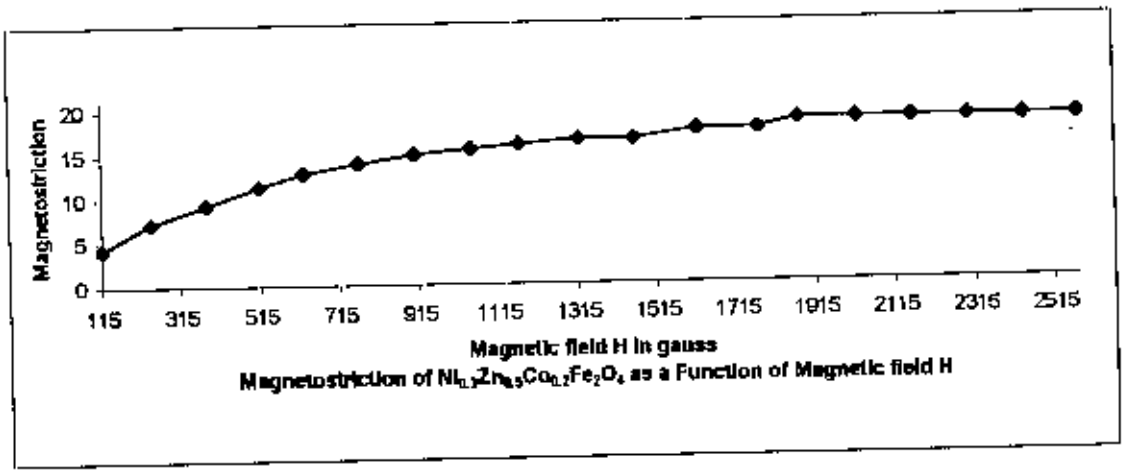

Magnetostriction of $Ni_{0.3}Zn_{0.5}Co_{0.2}Fe_2O_4$ as a Function of Magnetic field H

Fig.:6.2

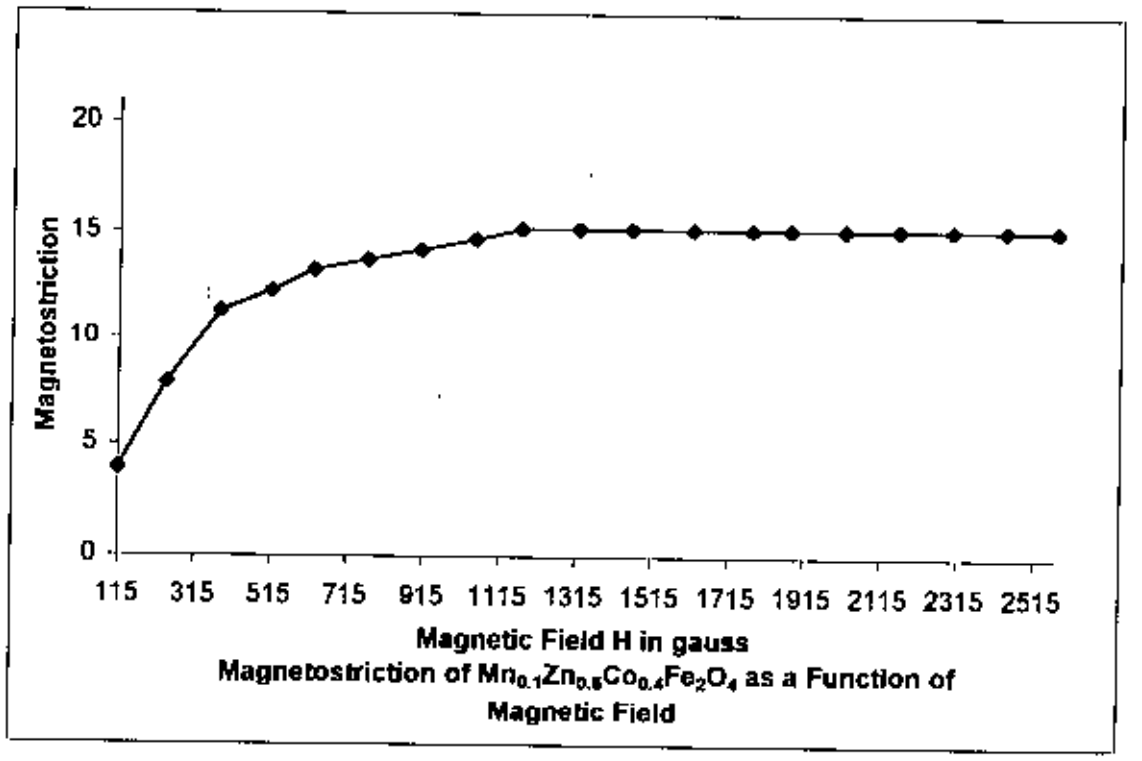

$\frac{\Delta l}{l} \times 10^{-6}$

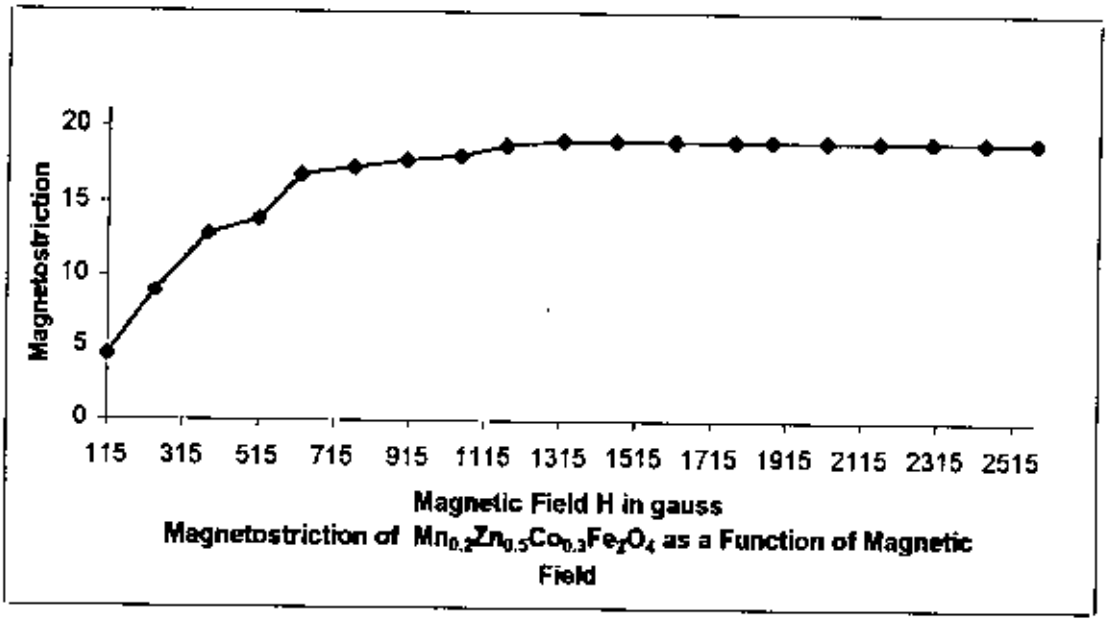

Fig.: 6.3

The mechanism of magnetostriction can be explained in the light of Neel's theory [6.1], by using a simple microscopic model. The model postulates certain properties of the energy of interaction of the neighboring atoms without any detail investigation of the directional dependence of the interaction. The justification of this assumption is found to be the agreement between the experimental and the calculated results. If r is the distance from the central atom to one of its neighbors, and Φ is the angle between the line of centers and the direction of the moment, the interaction energy can be expressed as

$$W(r,\cos\Phi)=g(r)+l(r)\left(\cos^2\Phi-\frac{1}{3}\right)+q(r)\left(\cos^2\Phi-\frac{6}{7}\Phi+\frac{3}{35}\right)+\ldots\ldots \qquad 6.3$$

If the interaction energy is a function of r, the crystal lattice must be deformed upon the generation of a ferromagnetic moment, because such an interaction tends to change the bond length depending on the bond direction. The first term g(r) is the exchange interaction term and plays an important role to the volume magnetostriction. The second term represents the dipole-dipole interaction, which depends on the direction of the magnetization. This is the main origin of saturation magnetostriction λ_s that we observed. Neglecting higher order terms one can express the pair energy term as

$$W(r,\Phi)=+l(r)\left(\cos^2\Phi-\frac{1}{3}\right) \qquad 6.4$$

When the specimen is strained its spin pair changes its bound direction as well as its boud length. The condition for the minimization of the total energy $E = E_{magnetic} + E_{elastic}$ is obtained by differentiating the total energy with respect to strain, and equating it to zero. From the condition of minimum energy, we can obtain the expression for magnetostrictive strain as $\frac{\Delta l}{l}=\frac{3}{2}\lambda_s(\cos^2\theta-1)$.

Since magnetostriction is an important factor in determining the permeability of a material, it is important to find the appropriate alloy composition for which the magnetostriction constant becomes minimum if one wants to find out a soft magnetic alloy.

From our experimental determination, as shown in figure 6.2 the ferrites with composition $Ni_{0.3}Zn_{0.5}Co_{0.2}Fe_2O_4$ has minimum magnetostriction. The maximum magnetostriction was found for $Ni_{0.1}Zn_{0.5}Co_{0.4}Fe_2O_4$. The reason for the variation of magnetostriction with the change of composition is assumed to be the varying contribution to magnetostriction from *Fe-* and *Ni-* atoms, which have +ve and -ve magnetostriction respectively as observed in their crystalline forms. The actual understanding of this compositional dependence of magnetostriction requires a complete quantum mechanical calculations of band structures of these ferrites systems.

The energy levels of the electron of the 3d-transition metals and alloys are the most exposed except for the 4f's-conduction electrons. These energy levels are perturbed due to overlapping of the 3d-shell's of the neighboring atoms. The effect of alloying ferromagnetic metals is to change in electronic structure. which in turn changes magnetostriction and other secondary effects of the resultant alloy. A magnetic material can thus be tailored if the effect of alloying on magnetostriction and magnetic anisotropy can be understood quantitatively. However, at the moment all calculation are found to be inexact due to the difficulty of treating different electron spin correlation functions exactly.

Magnetostriction arises from the spin-orbit interaction because, while the magnetization is determined by the exchange interaction between spins mostly, the exchange interaction being isotropic cannot contribute to the linear magnetostriction. Although it can contribute to volume magnetostriction. The unquenched part of the orbital moment which arises from the orbital electron motion can see the lattice. In order to reduce the electrostatic energy. Because of the spin-orbit interaction the spin and therefore the magnetization can see the lattice through the spin orbit-interaction. The mechanism gives rise to magnetic anisotropy. The materials will spontaneously strain to reduce the anisotropy energy so long the reduced of the anisotropy energy by this process do not exceed the corresponding increase in elastic energy.

The general mechanism of magnetostriction can be understood in terms of dipole-dipole interaction, which depends on the direction of magnetization. This interaction tends to change the bond length in different ways depending on the bond direction. The linear magnetostriction can be attributed to the rotation of this bond direction of magnetization, which is measured by rotating the magnetization direction, in our case from parallel position to perpendicular position by rotating the magnetic field.

6.2 Thermal expansion

Thermal expansion is an important parameter which reflects the nature of the binding energy and anharmonycity of the periodic motion of the constituent atoms under thermal excitation. The other theoretical interest is the nature of the binding energy and the potential well as a function of interatomic distance, which arises due to combined effet of the attractiveforce and the repulsive force. The technological application of magnetic materials make thermal expansion an important phenomena depending on the nature of the application. We sometimes prefer materials with high thermal expansion coefficient and sometimes material with low thermal expansion. In constructing devices by using magnetic materials, where change in dimension is undesirable under varied thermal environment, materials with low thermal expansion is preferable. For the use of ferrites as transformer core, low thermal expansion coefficient is desirable. Because thermal expansion may give rise to magnetostrictive noise. On the other hand when one uses materials for producing magnetostrictive tranducers, higher values of thermal expansion coefficient is desirable.

We measured the thermal expansion of the ferrite samples to find magnetic contribution to lattice energy. Thermal expansion depends on unharmonicity of the lattice atoms which are related to electronic and magnetic contributions. In our Ferrite samples which are magnetically soft, magnetic contributions play an important role to lattice energy.

We measured it by straingauge technique and got lattice strain from liquid Nitrogen temperature to room temperature. We measured the lattice strain that increased with increasing temperature gives rise to thermal expansion.

From figures6.4 and 6.5 we found thermal expansions of the series, $Ni_{0.1}Zn_{0.5}Co_{0.4}Fe_2O_4$, $Ni_{0.2}Zn_{0.5}Co_{0.3}Fe_2O_4$, $Ni_{0.3}Zn_{0.5}Co_{0.2}Fe_2O_4$ and of $Mn_{0.1}Zn_{0.5}Co_{0.4}Fe_2O_4$, and $Mn_{0.2}Zn_{0.5}Co_{0.3}Fe_2O_4$, respectively.

The linear thermal expansion coefficients are shown in figures6.6,6.7.6.8,6.9,and 6.10 for the ferrite samples. From these figures we see that thermal expansion coefficient is increasing from low temperature to room temperature which is quite expected. We estimated the average thermal expansion coefficients which are 3.19×10^{-6}, 2.37×10^{-6}, 2.66×10^{-6} for $Ni_{0.1}Zn_{0.5}Co_{0.4}Fe_2O_4$, $Ni_{0.2}Zn_{0.5}Co_{0.3}Fe_2O_4$, $Ni_{0.3}Zn_{0.5}Co_{0.2}Fe_2O_4$ and 1.51×10^{-6}, 1.71×10^{-6} for $Mn_{0.1}Zn_{0.5}Co_{0.4}Fe_2O_4$, $Mn_{0.2}Zn_{0.5}Co_{0.3}Fe_2O_4$ respectively. The method used for these measurements although quite straight forward, the values obtained have some uncertainties, because we could not control the temperature properly. However the estimated result show that these samples have low expansion coefficients. These values will be useful to make devices using these materials.

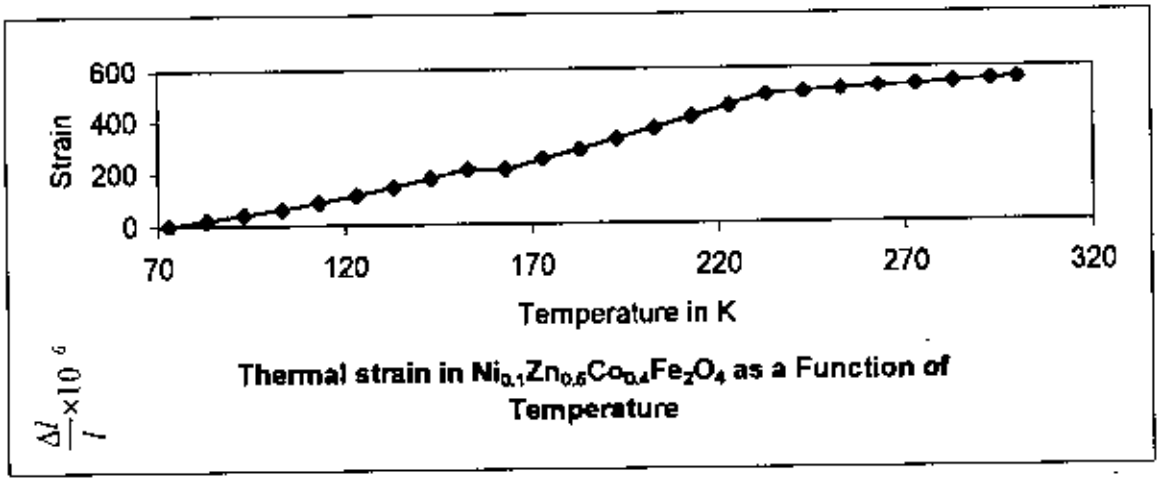

Thermal strain in $Ni_{0.1}Zn_{0.5}Co_{0.4}Fe_2O_4$ as a Function of Temperature

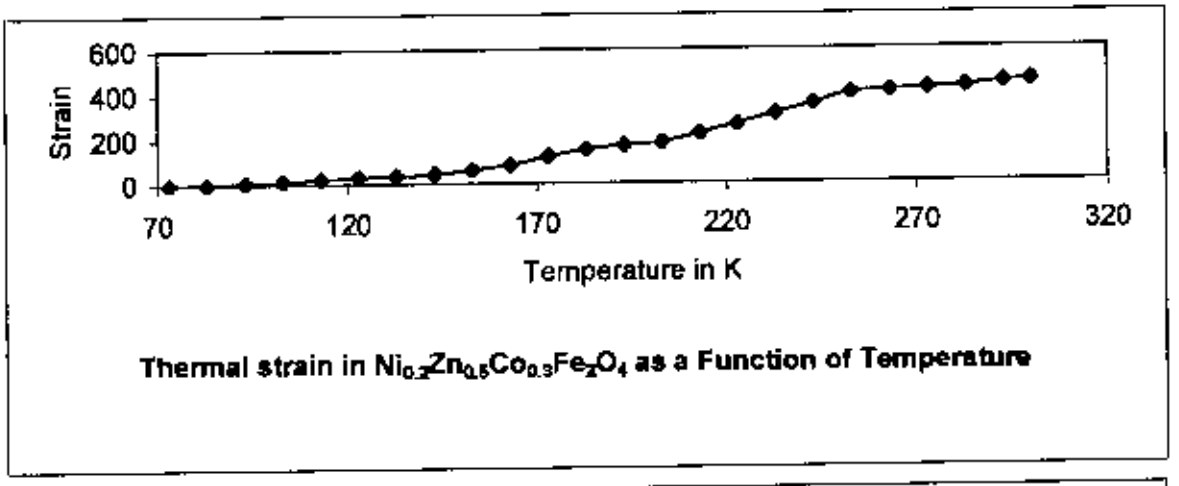

Thermal strain in $Ni_{0.2}Zn_{0.5}Co_{0.3}Fe_2O_4$ as a Function of Temperature

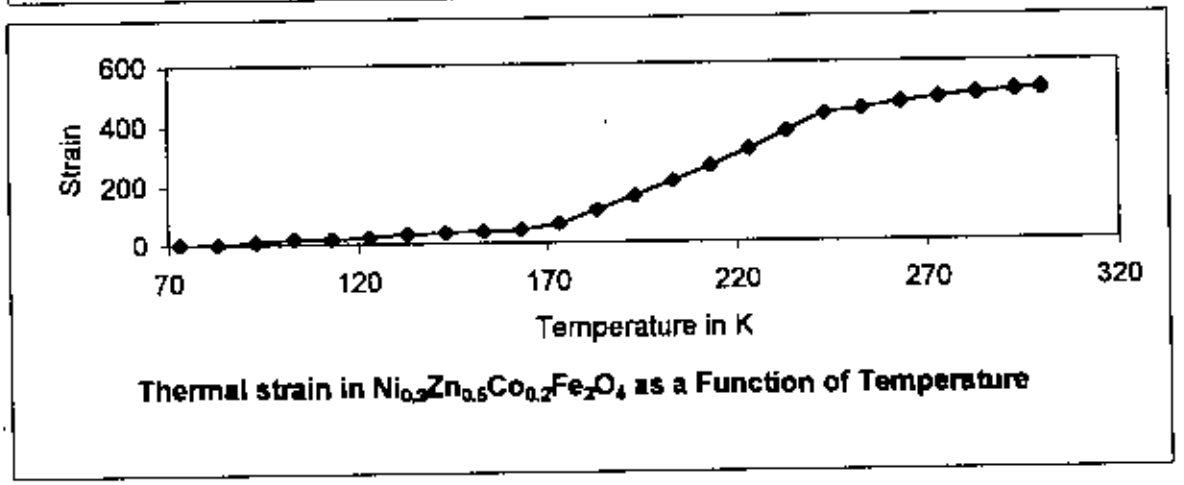

Thermal strain in $Ni_{0.3}Zn_{0.5}Co_{0.2}Fe_2O_4$ as a Function of Temperature

Fig.: 6.4

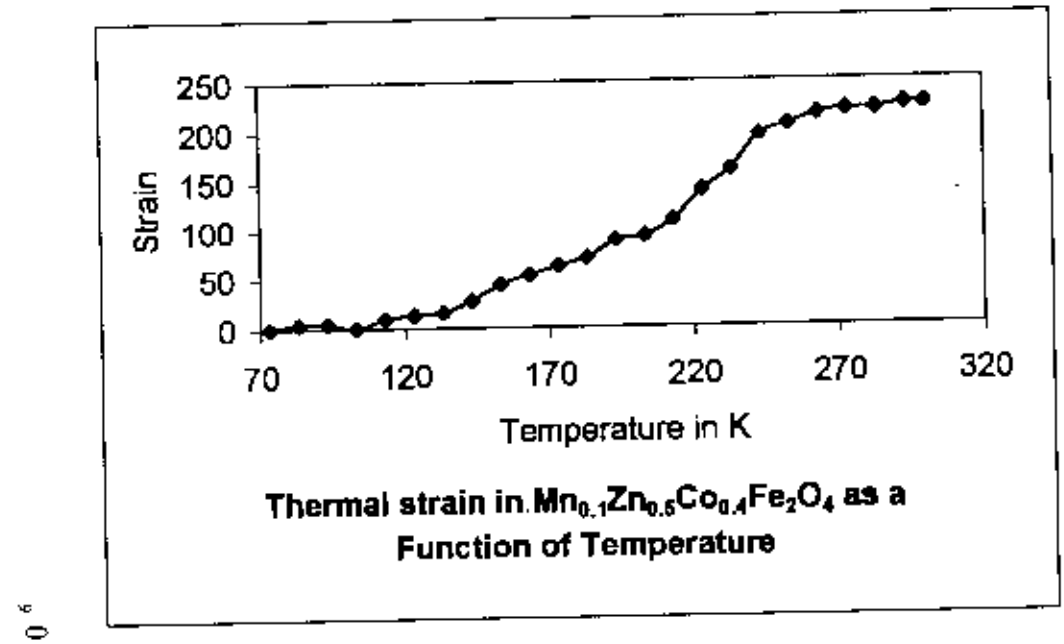

Thermal strain in $Mn_{0.1}Zn_{0.5}Co_{0.4}Fe_2O_4$ as a Function of Temperature

$\frac{\Delta l}{l} \times 10^{-6}$

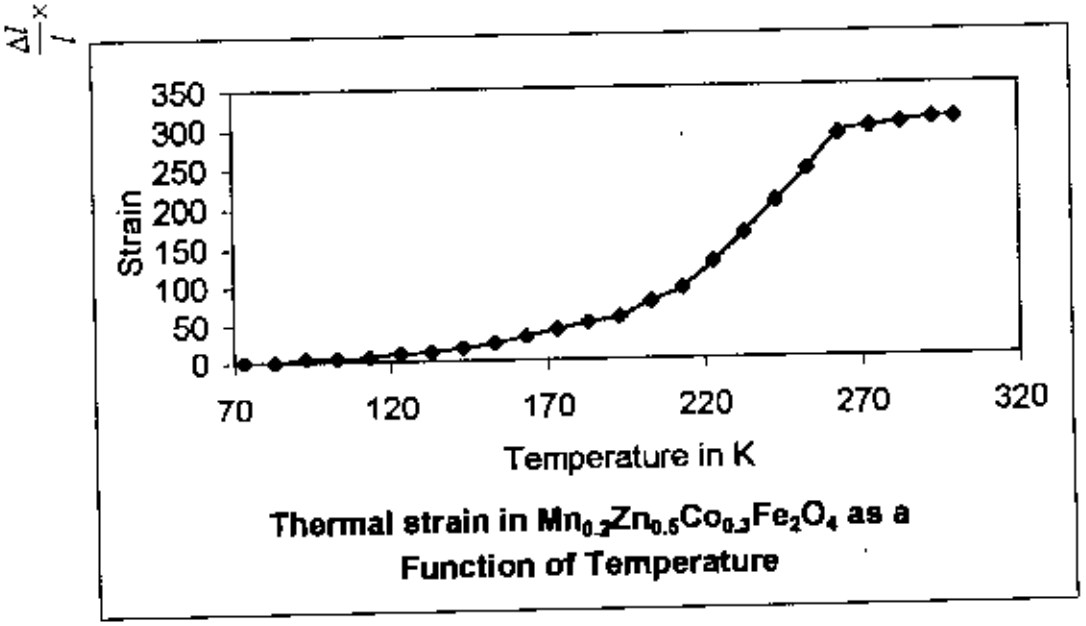

Thermal strain in $Mn_{0.2}Zn_{0.5}Co_{0.3}Fe_2O_4$ as a Function of Temperature

Fig.: 6.5

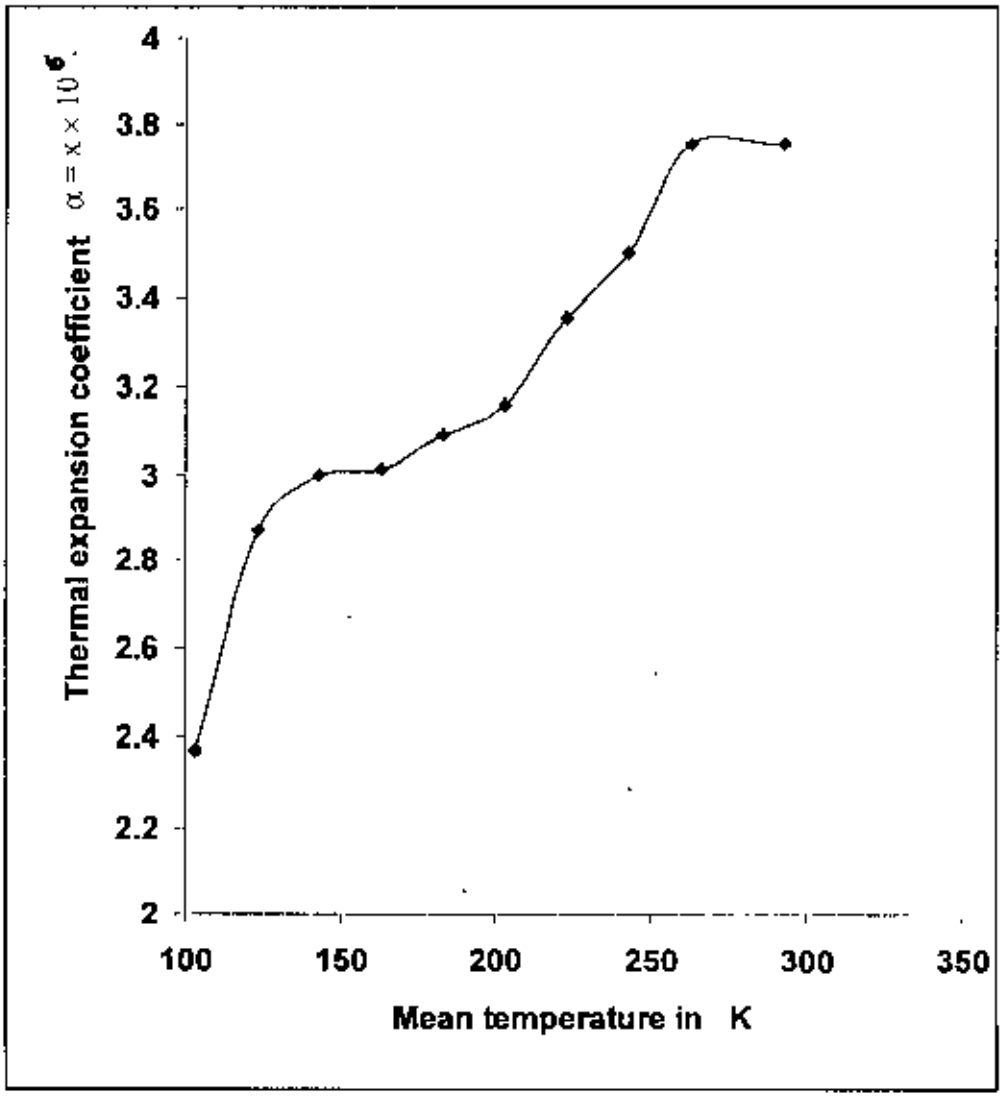

Figure 6.6: Thermal Expansion coefficient of $Ni_{0.1}$ $Zn_{0.5}$ $Co_{0.4}$ Fe_2 O_4 as a function of temperature.

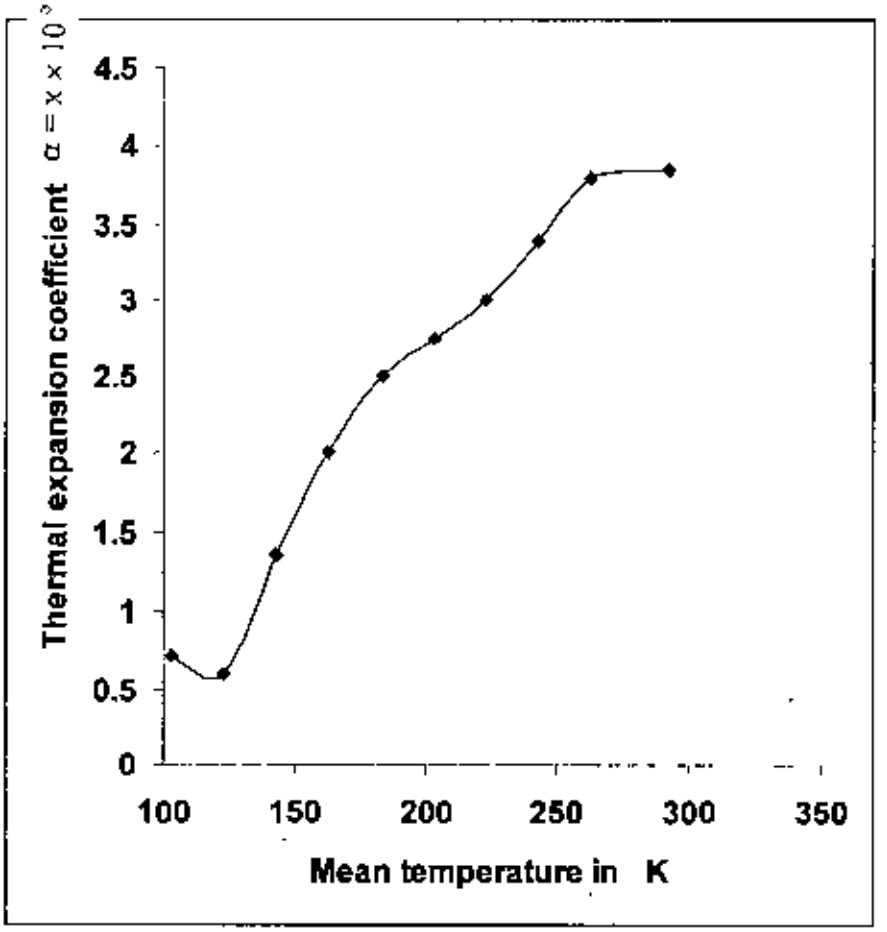

Figure 6.7: Thermal expansion coefficient of $Ni_{0.2}$ $Zn_{0.5}$ $Co_{0.3}$ Fe_2 O_4 as a function of temperature.

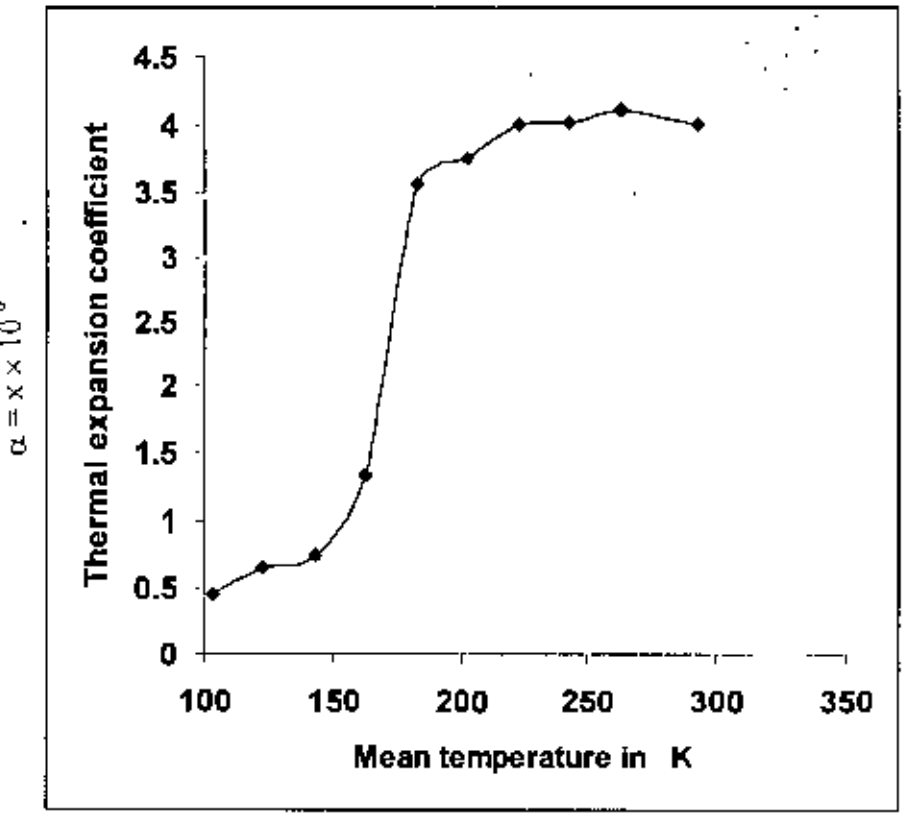

Figure 6.8: Thermal expansion coefficient of $Ni_{0.3}Zn_{0.5}Co_{0.2}Fe_2O_4$ as a function of temperature.

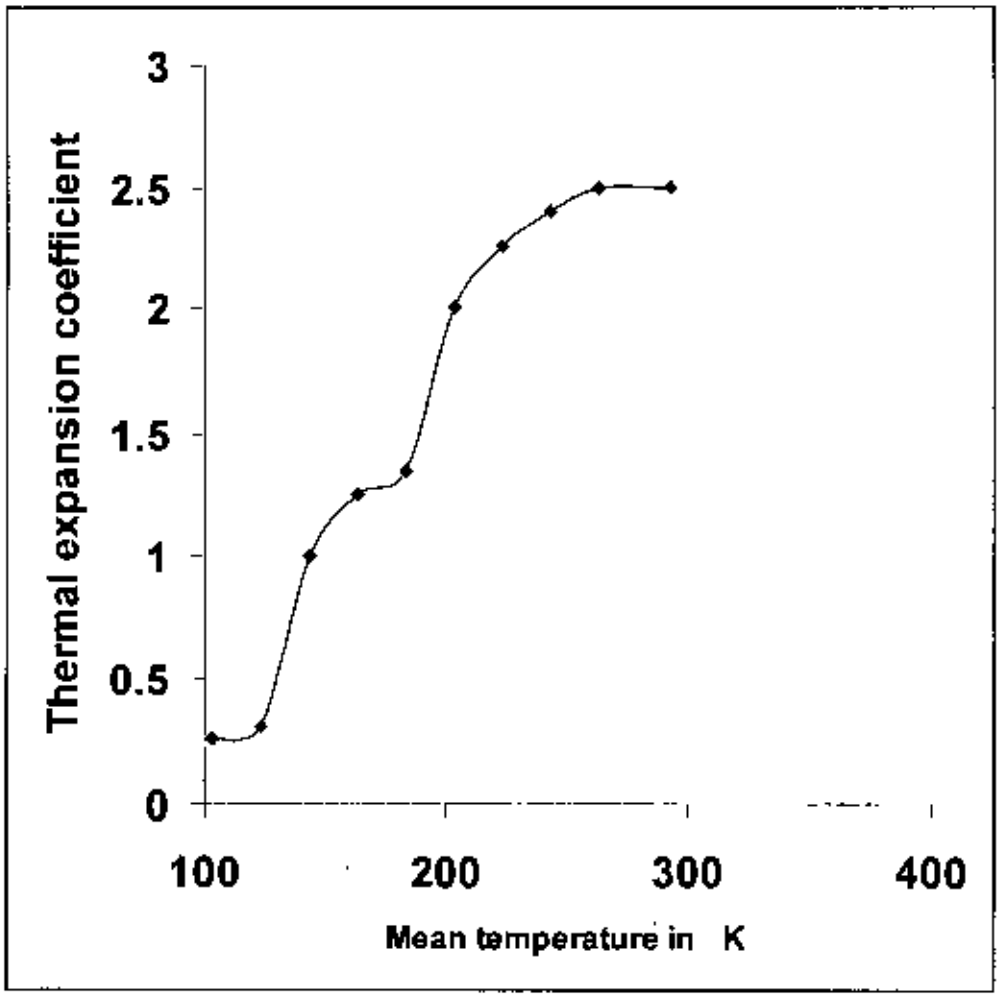

Figure 6.9: Thermal expansion coefficient of $Mn_{0.1}$ $Zn_{0.5}$ $Co_{0.4}$ Fe_2 O_4 as a function of temperature

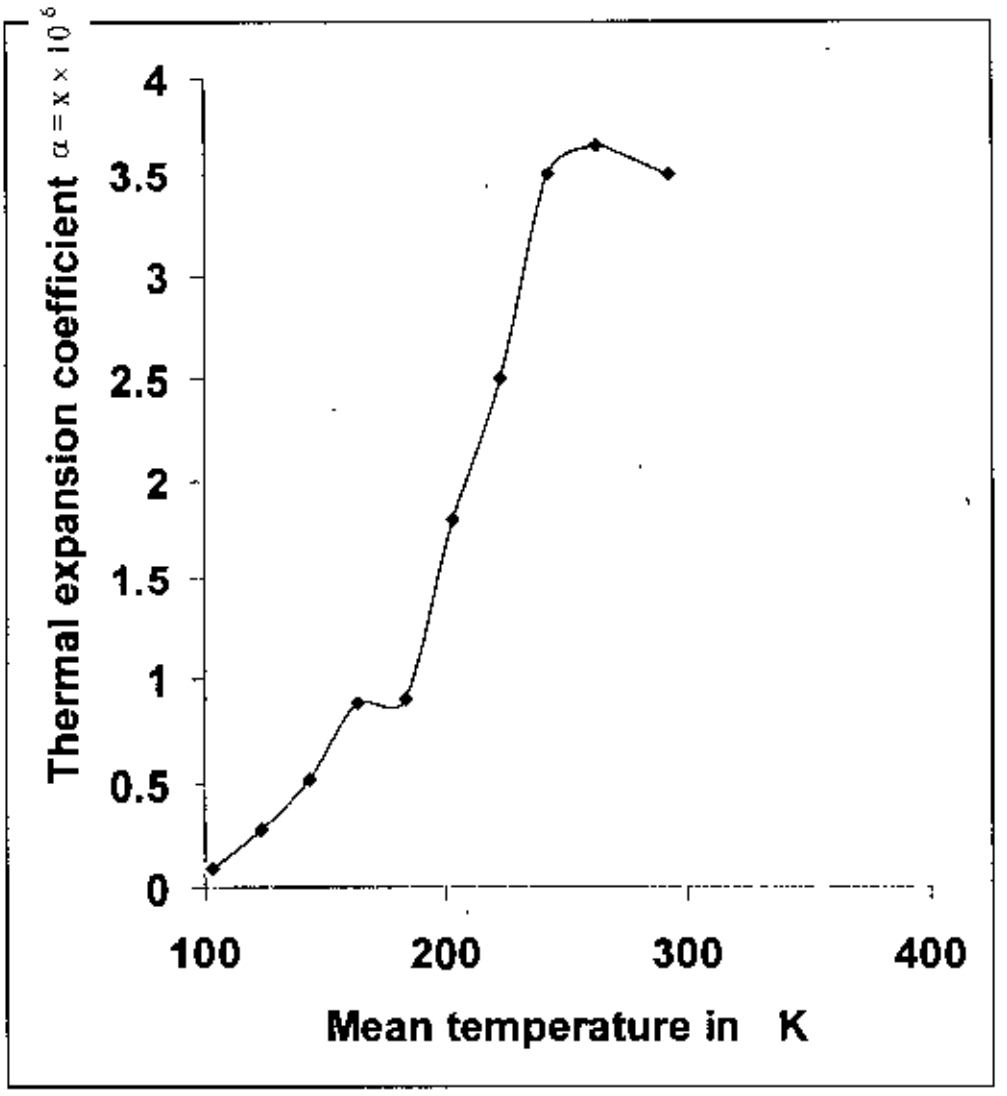

Figure 6.10: Thermal expansion coefficient of $Mn_{0.2}\ Zn_{0.5}\ Co_{0.3}\ Fe_2\ O_4$ as a function of temperature.

CHAPTER - VII

Conclusions

CHAPTER VII
CONCLUSIONS

New compositions of Co substituted Ni Zn and Mn Zn ferrites have been studied specially magnetostriction and thermal expansion. The observed values of magnetostriction are found to be 21×10^{-6}, 19.80×10^{-6} and 18.44×10^{-6} for $Ni_{0.1}\ Zn_{0.5}\ Co_{0.4}\ Fe_2O_4$, $Ni_{0.2}\ Zn_{0.5}\ Co_{0.3}\ Fe_2O_4$, $Ni_{0.3}\ Zn_{0.5}\ Co_{0.2}\ Fe_2O_4$ respectively. On the other hand we got the values of magnetostriction as 15.20×10^{-6} and 18.90×10^{-6} for $Mn_{0.1}\ Zn_{0.5}\ Co_{0.4}\ Fe_2O_4$, $Mn_{0.2}\ Zn_{0.5}\ Co_{0.3}\ Fe_2O_4$ respectively. From the results we could see that magnetostrictions of these two series of ferrite samples are very low. These compositions are therefore quite useful in making soft magnetic materials and can play an important role in making magnetic devices where dynamic flux change is necessary.

The study of thermal expansion which is another parameter of the ferrite samples measured, show that the materials have low thermal expansion coefficient We have used strain gauge technique for these measurements The strain gauge technique although, use for strain measurement and for magnetostriction measurement, had been used for the first time for thermal expansion by M.A. Asgar [7.1]. The thermal expansion coefficients show that these materials can conveniently be used in situation, where thermal changes are involved.

REFERENCES

Chapter - 1

References:

1.1 T.M. Clark, B.J. Evans, J. Magn. Magn. Maters. 177-181 (1998), 237.
1.2 J. Muller, A. Collomb, J. Magn. Magn. Mater. 103 (1992) 194.
1.3 Adam Bienkowski J. Magn. Magn. Maters. 112 (1992) 143.
1.4 H. A. Brooks, J. Appl. Phys., 47 (1976) 334.
1.5 A. J. Moses, IEEE Trans. Magn. MAG-14 (1978) 353.
1.6 E. De Lacheisserie, J. Magn. Magn. Mater. 13 (1979) 304.
1.7 A. N. Bazhan, V. N. Bevz. J. Magn. Magn. Maters 140-144 (1995) 1799.
1.8 A. N. Bazhan. Sov. Phys. JETP 38 (1974) 1238.
1.9 A. N. Bazhan. V. N. Bevz and S. V. Petrov, Sov. Phys. JEPT 67 (1988) 779.
1.10 G. Polatsek, O. Entin-Wohlman and R. Orback. J. Physique coll. C8, suppl. 12, 48 (1988) 1191.
1.11 E. P. Shender, Sov. Phys. JETP 48 (1978) 175.
1.12 K. I. Kobayashi, et al J. Magn. Magn. Maters. 104-107 (1992) 413.
1.13 Y. Sakaki and S. I. Imagi, IEEE Trans. Magn. MAG-17 (1981) 1478.
1.14 M. Nogues. et al, J. Magn. Magn. Maters. 104-107 (1992) 415.
1.15 M. A. Asgar, M. A. Hakim. M. A. Mazid, Journal of Bangladesh Academy of Sciences 20(2) (1996), 237.

Chapter - 2

References:

2.1 J. Born, Von, Karman; J. Low, Temp. Phys. 27 (5-6) 837-50, (1977), Theory of thermal expansion and lattice vibrations in crystals.

2.2 Major, J, Minhaly, L. G; and Tichy, G; Tr. Mezdhunar, Konf. Magn, (1973). 3, 224-9 ("Publ. Nauka" Moscow, USSR, 1974) Thermal expansion coefficient and spedivic heat of nickel near the curie point.

2.3 Shmakova, E. S., Lebedev, Yu, N, d Nagronyi V.G, Khim Tverd. Topl. 125-3 (1977), (euss) change in the interlayer spacing in the structure of carbon materials at low temperature.

2.4 E.W. Lee and M.Ali Asgar, Physical Riview letter voll. 22 No. 26, (1969).

2.5 Tolpadi, s, Indian J. Pure. Appl. Phys. 14, 315-16 (1976), Isobaric Gruneisen Parameter of Alkali halide crystal.

2.6 Bill and Pullan; J. Appl. Phys. 47(II), 5115 (1976); High temperature thermal expansion of iridium.

2.7 Kittel, Solid State Physics, J. M. M. Vol-11, No. 20, (1968).

2.8 Shinozaki, akajima, Seya, K. and Sumino, Y. Phys. chem. Miner. 3, (2), 111-15, (1978), Thermal expansion of single crystal tephorite.

2.9 Yahagi Mashito, J. Phys. Soc. Japan, 43 (6) 2097, (1977), A study on thermal expansion of lithium-aluminium-indium ($LiAl_{1-x}In_x$) system.

Chapter - 3

References:

3.1 M.A. Asgar, Proceeding of the international conference on physics and energy for development, Dhaka, 26-29, Jan, 153p (1985).

3.2 J.H. Van Vleck phys. Rev. 52, 1178 (1938).

3.3 Cochrane, R. W., R. Harris and M. Plischke, 1974, J. Non-Cryst. solids 15, 239.

3.4 Fähnel, M., and T. Egami, 1982, J. Appl. Phys. 53, 2319.

3.5 Suzuki, Y., and T. Egami, 1983, J. Magn. & Magn. Mater. 31-34, 1459.

3.6 Lachowicz, H. K., and H. Szymczak, 1984, J. Magn. & Magn. Mater. 41, 327.

3.7 O'Handley, r. C., and N. J. Grant, 1985, Proceedings on Rapidly quenched Metals, eds. S. Steeb and H. Warlimont (North-Holland, Amsterdam) p-1125.

3.8 Furthmüller, J., M. Fähnle and G. Herzer, 1986, J. Phys. F 16, L255.

3.9 Furthmüller, J., M. Fähnle and G. Herzer, 1987a, J. Magn. & Magn. Mater, 69, 79.

3.10 Furthmüller, J., M. Fähnle and G. Herzer, 1987b, J. Magn. & Magn. Mater, 69, 89.

3.11 Szymczak, H., 1987, J. Magn. & Magn. Mater, 67, 227.

3.12 M. Fähnle and Furthmüller, J.,1988, J. Magn. & Magn. Mater, 72, 6.

3.13 M. Fähnle and Furthmüller, J.,1989, Phys. Status Solidi a 116, 819.

3.14 Pawellek, R., J. Furthmüller and M. Fähnel, 1988, J. Magn. & Magn. Mater, 75, 225.

3.15 Suzuki, Y., and N. Ohta, 1988, J. Appl. Phys. 63, 3633.

3.16 L. Neel, Ann de Physique, 3, 137 (1948).

3.17 W.P. Mason and J. A. Lewies, Phys. Rev., 94, 1439 (1954).

Chapter - 4

References:

4.1 HILPERT. S., Genetische and konstitutive Zusammen-hänge in den magnetischen Eigenschaften bei Ferriten and Eisenoxyden, Ber, disch, chem. Ges., 42, 2248, (1909).

4.2 FORESTIER, H., "Transformations magnetiques du sesquioxide de fer, de ses solutions solides, et des ses combinations ferromagnetiques", Ann. Chim., Xe Serie, IX, 316 (1928).

4.3 KATO, V, and TAKEI, T., "Permanent oxide magnet and its characteristics", J. Insin. elect. Engrs. Japan, 53, 408, (1933).

4.4 KAWAJ, N., "Formation of a solid solution between some ferrites", J. Sec. chem. Ind. Japan, 37, 392, (1934).

4.5 SNORK, J. L., "Magnetic and electrical properties of the binary systems MO Fe_2O_3, Physica, Amsterdam. 3, 463. (1936).

4.6 SNOEK. J. L., New developments in ferromagnetic materials, Elsevier Publishing Company, Inc. New York Amsterdam, (1947).

4.7 POLDER, D., Ferrite materials, Proc. Instn elect. Engrs. 97, Part II, 246, (1950).

4.8 OWENS, C. D., A survey of tghe properties and applications of ferrites below micrewave frequencies, Proc. Inst. Radio Engrs. 44, 1234, (1956).

4.9 SNELLING, I. C., Properties of ferrites in relation to their applications, Proc. Br. Ceram. Soc. 2, 151, (1964).

4.10 ERZBERGER, P., Correlation of partial size with other physical properties of iron oxides for ferrite synthesis, Proc. Brit. Ceram. Soc. 2, 19, (1964).

4.11 SWALLOW, D. and ZORDAN, A.K. The babrication of ferrites. Proc. Br. Ceram Soc. 2,1. (1964).

4.12 GUILLAUD, C. and PAULUS, M. Permeabilite initiable at grosser der grains dan less ferrites de magnanese zinc, CR. Acad. Sci. Paris, 242, 2525, (1956).

4.13 STUUTS, A.L., Microstructural considerations in ferromagnetic ceramics, Proc. 3rd. Univ. Calif. Bericeley, (June 1966).

Chapter - 5

References:

5.1 M. A. Asgar, Proceeding of the International Conference on Physics and Energy for Development, Dhaka, 26-29 Jan., 153p (1985).

5.2 M.A. Asgar, Ph.D. Thesis, University of Southampton (1970).

5.3 H. Nagaoka, Phil. Mag. 37. 131 (1894).

5.4 H.P. Rooksby and B. T. M. Willis, Nature. 172, 1054 (1953).

5.5 C.M. Hurd, Hall Effect in Metals and Alloys, Plenum Press, New York, (1972).

5.6 A. K. Majumdar, L. Berger, Phys. Rev. B7, 4203 (1973).

5.7 J. A. Rayne, R. A. Levy, in: R. Levy, R. Hasegawa (Eds.), Amorphous Magnetism II, Plenum Press, New York, (1977)

5.8 R. C. O'Handlyey, Phys. Rev. B 18, 2577 (1978).

Chapter VI

References:

6.1 L. Neel, Ann de Physique, 3, 137 (1948).

Chapter VII

References:

7.1 E.W. Lee and M.Ali Asgar, Physical Riview letter voll. 22 No. 26, (1969).

APPENDIX

Table: I

Data for Magnetic Field Strength

Field Current (Amp)	Fluxmeter Reading I(+)	Fluxmeter Reading I(-)	Average Deflection	Magnetic field (Gauss)
0.2	10	13	11.5	115
0.4	22	26	24.0	240
0.6	35	41	38.0	380
0.8	48	54	51.0	514
1.0	60	65	62.5	625
1.2	73	80	76.5	765
1.4	86	95	90.5	905
1.6	100	110	105.0	1050
1.8	113	121	117.0	1170
2.0	127	137	132.0	1320
2.2	142	150	146.0	1460
2.4	155	169	162.0	1620
2.6	169	186	177.5	1775
2.8	183	192	187.5	1875
3.0	197	207	202.0	2020
3.2	211	221	216.0	2160
3.4	224	236	230.0	2300
3.6	239	249	244.0	2440
3.8	252	263	257.5	2575
4.0	268	277	272.5	2725
4.2	281	298	289.5	2895
4.4	295	304	299.5	2995
4.6	308	318	313.0	3130
4.8	322	331	326.5	3265
5.0	335	345	340.0	3400
5.2	350	356	353.0	3530
5.4	362	369	365.5	3655
5.6	376	381	378.5	3785
5.8	391	394	392.5	3925
6.0	405	406	405.5	4055
6.2	416	416	416.0	4160

Table: II

Data for Calibration of the D.C. Bridge

Gauge Factor: G = 2.04
Bridge Current: 1.55 mA

Deflection in Nanovoltmeter	$\Delta R/R \times 10^{-6}$
0	0
4	1.6
7	3.5
8	5.5
9	7.4
10	9.4
11	11.4
13	13.5
15	15.5
20	17.8
29	19.8
33	22.0
38	24.4
43	26.6
51	29.2
70	31.5
71	33.8
72	36.3
73	38.6
74	40.9
75	43.4
76	45.7
76	48.0

Table: III

Variation of Bridge Sensitivity with Bridge Current

Gauge Factor, G = 2.04
$\Delta R/R = 40\times10^{-6}$

Current	Deflection
0	0
0.18393	2.0
0.20369	3.5
0.20388	5.5
0.22871	7.5
0.26048	9.3
0.30241	11.3
0.36049	13.4
0.44608	15.5
0.58516	17.5
0.84984	20.0
1.55198	22.2
1.69082	24.5
1.85796	26.8
2.06203	28.9
2.08459	31.2
2.08457	33.5
2.10789	36.0
2.13192	38.1
2.15642	40.7
2.1815	43.0
2.18668	45.4
2.19939	47.7

Table: IV

Variation of magnetostriction with the angle of Field Bridge current: 1.546mA, gauge factor: 2.04 per deflection

$\Delta R/R = 4.39\times10^{-6}$

Magnet position	Nanovolt meter reading	Magnetostriction $[\lambda=\frac{3}{2}\lambda_s(\cos^2\theta-\frac{1}{3})$ $=\Delta l/l= 1/G\Delta R/R\times10^{-6}]$
0	0	0
10	0.75	1.61
20	0.75	1.61
30	1.00	2.15
40	1.5	3.22
50	2.2	4.75
60	4	8.60
70	6	12.90
80	7	15.06
90	8.5	18.29
110	10.0	21.50
120	9.5	20.44
130	9.0	19.36
140	8.75	18.82
150	7.50	16.14
160	5.00	10.75
170	4.00	8.60
180	2.50	5.37
190	1.00	2.15
200	1.25	2.70
210	2.00	4.30
220	3.00	6.45
230	4.00	8.60
240	4.00	8.60
250	6.00	12.90
260	7.00	15.06
270	8.00	17.21
280	9.00	19 36
290	10.00	21 50
300	9.00	19.36
310	8.00	17.21
320	7.00	15.06
330	6.00	12.91
340	5.00	10.75
350	4.00	8.60
360	3.00	6.45

TABLE V

Table for Magnetostriction
Sample: $Ni_{0.1}Zn_{0.5}Co_{0.4}Fe_2O_4$
Gauge Factor G=2.04
Angle θ = 20° [Perpendicular Position]
θ =110° [Parallel]
$\Delta R/R = 4.39\times10^{-6}$

Field Current [F]	Magnetic Field Strength (Gauss) [H]	ΔR/R	Magnetostriction $[\lambda=\frac{3}{2}\lambda_s(\cos^2\theta-\frac{1}{3})$ $=\Delta l/l= 1/G\Delta R/R\times10^{-6}]$
0.2	115	2	4.30
0.4	240	3	6.45
0.6	380	5	9.68
0.8	514	5.2	11.19
1.0	625	6.5	13.98
1.2	765	7	15.05
1.4	905	7.5	16.14
1.6	1050	7.7	17.00
1.8	1170	8.5	18.30
2.0	1320	9.0	19.30
2.2	1460	9.0	19.36
2.4	1620	9.2	19.80
2.6	1775	9.4	20.25
2.8	1875	9.5	20.25
3.0	2020	10.0	21.00
3.2	2160	10.0	21.00
3.4	2300	10.0	21.00
3.6	2440	10.0	21.00
3.8	2575	10.0	21.00

TABLE VI

Table for Magnetostriction
Sample: $Ni_{0.2}Zn_{0.5}Co_{0.3}Fe_2O_4$
Gauge Factor G=2.04
Angle θ = 20° [Perpendicular Position]
θ =110° [Parallel Position]
$\Delta R/R = 4.04\times10^{-6}$

Field Current [F]	Magnetic Field Strength (Gauss) [H]	ΔR/R	Magnetostriction $[\lambda=\frac{3}{2}\lambda_s(\cos^2\theta-\frac{1}{3})$ $=\Delta l/l= 1/G\Delta R/R\times10^{-6}]$
0.2	115	2	3.96
0.4	240	3	5.94
0.6	380	5	7.92
0.8	514	5.2	8.91
1.0	625	6.5	10.91
1.2	765	7	10.90
1.4	905	7.5	11.88
1.6	1050	7.7	12.87
1.8	1170	8.5	13.37
2.0	1320	9.0	13.86
2.2	1460	9.0	15.85
2.4	1620	9.2	16.84
2.6	1775	9.4	17.82
2.8	1875	9.5	18.82
3.0	2020	10.0	19.80
3.2	2160	10.0	19.80
3.4	2300	10.0	19.80
3.6	2440	10.0	19.80
3.8	2575	10.0	19.80

TABLE VII

Table for Magnetostriction
Sample: $Ni_{0.3}Zn_{0.5}Co_{0.2}Fe_2O_4$
Gauge Factor G=2.04
Angle θ = 20° [Perpendicular Position]
θ =110° [Parallel]
$\Delta R/R = 4.39\times10^{-6}$

Field Current [F]	Magnetic Field Strength (Gauss) [H]	ΔR/R	Magnetostriction $[\lambda=\frac{3}{2}\lambda_s(\cos^2\theta-\frac{1}{3})$ $=\Delta l/l= 1/G\Delta R/R\times10^{-6}]$
0.2	115	2	4.10
0.4	240	3.5	7.17
0.6	380	4.5	9.22
0.8	514	5.5	11.27
1.0	625	6.25	12.80
1.2	765	6.75	13.84
1.4	905	7.25	14.86
1.6	1050	7.50	15.37
1.8	1170	7.75	15.88
2.0	1320	8.00	16.40
2.2	1460	8.00	16.40
2.4	1620	8.50	17.42
2.6	1775	8.50	17.42
2.8	1875	9.00	18.45
3.0	2020	9.00	18.45
3.2	2160	9.00	18.45
3.4	2300	9.00	18.45
3.6	2440	9.00	18.45
3.8	2575	9.00	18.45

TABLE VIII

Table for Magnetostriction
Sample: $Mn_{0.1}Zn_{0.5}Co_{0.4}\ Fe_2O_4$
Gauge Factor G=2.04
Angle θ = 20° [Perpendicular Position]
θ =110° [Parallel]
$\Delta R/R = 4.39\times10^{-6}$

Field Current [F]	Magnetic Field Strength (Gauss) [H]	ΔR/R	Magnetostriction $[\lambda=\frac{3}{2}\lambda_s(\cos^2\theta-\frac{1}{3})$ $=\Delta l/l= 1/G\Delta R/R\times10^{-6}]$
0.2	115	2	3.92
0.4	240	4	7.84
0.6	380	5.75	11.27
0.8	514	6.25	12.25
1.0	625	6.75	13.25
1.2	765	7.00	13.72
1.4	905	7.25	14.20
1.6	1050	7.50	14.70
1.8	1170	7.75	15.20
2.0	1320	7.75	15.20
2.2	1460	7.75	15.20
2.4	1620	7.75	15.20
2.6	1775	7.75	15.20
2.8	1875	7.75	15.20
3.0	2020	7.75	15.20
3.2	2160	7.75	15.20
3.4	2300	7.75	15.20
3.6	2440	7.75	15.20
3.8	2575	7.75	15.20

TABLE IX

Table for Magnetostriction
Sample: $Mn_{0.2}\ Zn_{0.5}Co_{0.3}\ Fe_2O_4$
Gauge Factor G=2.04
Angle θ = 10° [Perpendicular Position]
θ =100° [Parallel]
$\Delta R/R = 4.39\times10^{-6}$

Field Current [F]	Magnetic Field Strength (Gauss) [H]	ΔR/R	Magnetostriction $[\lambda=\frac{3}{2}\lambda_s(\cos^2\theta-\frac{1}{3})$ $=\Delta l/l= 1/G\Delta R/R\times10^{-6}]$
0.2	115	2.25	4.45
0.4	240	4.50	8.91
0.6	380	6.50	12.87
0.8	514	7.00	13.86
1.0	625	8.5	16.84
1.2	765	8.75	17.32
1.4	905	9.00	17.82
1.6	1050	9.25	18.13
1.8	1170	9.50	18.81
2.0	1320	9.75	19.11
2.2	1460	9.75	19.11
2.4	1620	9.75	19.11
2.6	1775	9.75	19.11
2.8	1875	9.75	19.11
3.0	2020	9.75	19.11
3.2	2160	9.75	19.11
3.4	2300	9.75	19.11
3.6	2440	9.75	19.11
3.8	2575	9.75	19.11

TABLE X

DATA FOR THERMAL EXPANSION

Sample: $Ni_{0.1}Zn_{0.5}Co_{0.4}Fe_2O_4$
Gauge Factor G=2.04
$\Delta R/R = 39.48\times10^{-6}$

Thermo emf in my	Temperature in ^0K	Nanovoltmeter Deflection	Thermal Strain $[\Delta 1/1=1/G\ \Delta R/R\times10^{-6}]$	Mean Temperature in ^0K	Linear thermal expansion coefficient $\alpha = x\times10^{-6}/^0K$
-5.53	73	0	0	103	2.37
-5.38	83	0	19.35	123	2.87
-5.20	93	0.24	40.00	143	3.00
-5.02	103	0.30	62.25	163	3.01
-4.82	113	0.60	87.50	183	3.09
-4.60	123	0.75	114.00	203	3.16
-4.38	133	0.90	144.00	223	3.35
-4.14	143	1.10	176.00	243	3.50
-3.84	153	1.57	209.00	263	3.75
-3.62	163	2.07	211.25	293	3.75
-3.35	173	3.05	247.50		
-3.06	183	3.75	285.00		
-2.77	193	4.27	325.00		
-2.46	203	4.52	366.00		
-2.14	213	5.51	408.25		
-1.81	223	6.53	451.50		
-1.47	233	7.65	495.00		
-1.11	243	8.80	505.00		
-0.75	253	10.00	515.25		
-0.38	263	10.25	526.00.		
0	273	10.43	530.00		
.39	283	10.67	540.50		
.79	293	11.12	550.25		
1.09	300	11.38	555.00		

TABLE XI

DATA FOR THERMAL EXPANSION

Sample: $Ni_{0.2}Zn_{0.5}Co_{0.3}Fe_2O_4$
Gauge Factor G=2.04
$\Delta R/R = 40\times10^{-6}$

Thermo emf in my	Temperature in ^0K	Nanovoltmeter Deflection	Thermal Strain $[\Delta1/1=1/G\ \Delta R/R\times10^{-6}]$	Mean Temperature in ^0K	Linear thermal expansion coefficient $\alpha = x\times10^{-6}/^0K$
-5.53	73	0	0	103	.71
-5.38	83	0	0	123	.60
-5.20	93	0.24	9.80	143	1.35
-5.02	103	0.36	12.00	163	2.00
-4.82	113	0.60	24.00	183	2.50
-4.60	123	0.75	30.00	203	2.75
-4.38	133	0.9	36.00	223	3.00
-4.14	143	1.10	44.00	243	3.40
-3.84	153	1.57	63.00	263	3.80
-3.62	163	2.07	83.00	293	3.85
-3.35	173	3.05	122.00		
-3.06	183	3.79	151.90		
-2.77	193	4.27	171.00		
-2.46	203	4.52	181.00		
-2.14	213	5 51	220.50		
-1.81	223	6.53	261.50		
-1.47	233	7.65	306.00		
-1.11	243	8.80	352 00		
-0.75	253	10.00	400.00		
-0.38	263	10.25	410.00		
0	273	10.43	417.25		
.39	283	10.67	427.00		
.79	293	11.12	445.00		
1.09	300	11.38	455.00		

TABLE XII

DATA FOR THERMAL EXPANSION

Sample: $Ni_{0.3}Zn_{0.5}Co_{0.2}Fe_2O_4$
Gauge Factor G=2.04
$\Delta R/R = 33.36\times10^{-6}$

Thermo emf in my	Temperature in ^0K	Nanovoltmeter Deflection	Thermal Strain [$\Delta l/l = 1/G\ \Delta R/R\times10^{-6}$]	Mean Temperature in ^0K	Linear thermal expansion coefficient $\alpha = x\times10^{-6}/^0K$
-5.53	73	0	0	103	0.45
-5.38	83	0	0	123	0.66
-5.20	93	0.26	8.91	143	0.75
-5.02	103	0.53	17.82	163	1.34
-4.82	113	0.53	17.82	183	3.55
-4.60	123	0.66	22.27	203	3.75
-4.38	133	0.93	31.19	223	4.00
-4.14	143	1.06	35.64	243	4.01
-3.84	153	1.19	40.00	263	4.10
-3.62	163	1.34	45.00	293	4.00
-3.35	173	2.00	66.85		
-3.06	183	3.33	111.35		
-2.77	193	4.73	158.00		
-2.46	203	6.25	208.50		
-2.14	213	7.79	260.00		
-1.81	223	9.42	314.00		
-1.47	233	11.15	372.25		
-1.11	243	12.94	432.00		
-0.75	253	13.48	450.00		
-0.38	263	14.08	470.00		
0	273	14.53	485.00		
.39	283	14.83	495.00		
.79	293	15.15	505.25		
1.09	300	15.25	510.00		

TABLE XIII

DATA FOR THERMAL EXPANSION

Sample: $Mn_{0.1}Zn_{0.5}Co_{0.4}Fe_2O_4$
Gauge Factor G=2.04
$\Delta R/R = 36.36\times10^{-6}$

Thermo emf in my	Temperature in ^0K	Nanovoltmeter Deflection	Thermal Strain [$\Delta l/l = 1/G\ \Delta R/R\times10^{-6}$]	Mean Temperature in ^0K	Linear thermal expansion coefficient $\alpha = x\times10^{-6}/^0K$
-5.53	73	0	0	103	0.25
-5.38	83	0.12	4.45	123	0.30
-5.20	93	0.12	4.45	143	1.00
-5.02	103	0	0	163	1.25
-4.82	113	0.25	9.45	183	1.35
-4.60	123	0.37	13.50	203	2.00
-4.38	133	0.42	15.50	223	2.25
-4.14	143	0.77	28.00	243	2.40
-3.84	153	1.22	44.55	263	2.50
-3.62	163	1.47	53.46	293	2.50
-3.35	173	1.71	62.37		
-3.06	183	1.96	71.28		
-2.77	193	2.46	89.50		
-2.46	203	2.58	94.00		
-2.14	213	3.02	110.00		
-1.81	223	3.85	140.00		
-1.47	233	4.40	160.00		
-1.11	243	5.36	195.00		
-0.75	253	5.63	205.00		
-0.38	263	5.92	215.50		
0	273	6.05	220.00		
.39	283	6.05	220.00		
.79	293	6.18	225.00		
1.09	300	6.18	225.00		

TABLE XIV

DATA FOR THERMAL EXPANSION

Sample: $Mn_{0.2}Zn_{0.5}Co_{0.3}Fe_2O_4$
Gauge Factor G=2.04
$\Delta R/R = 36.36\times10^{-6}$

Thermo emf in my	Temperature in ^0K	Nanovoltmeter Deflection	Thermal Strain [$\Delta l/l = l/G\ \Delta R/R\times10^{-6}$]	Mean Temperature in ^0K	Linear thermal expansion coefficient $\alpha = x\times10^{-6}/^0K$
-5.53	73	0	0	103	0.09
-5.38	83	0	0	123	0.28
-5.20	93	0.12	4.45	143	0.52
-5.02	103	0.12	4.45	163	0.88
-4.82	113	0.17	6.25	183	0.90
-4.60	123	0.27	10.00	203	1.80
-4.38	133	0.33	12.00	223	2.50
-4.14	143	0 47	17.25	243	3.50
-3.84	153	0.61	22.50	263	3.65
-3.62	163	0.85	31.00	293	3.50
-3.35	173	1.10	40.25		
-3.06	183	1.34	49.00		
-2.77	193	1.57	57.00		
-2.46	203	2.04	76.00		
-2.14	213	2.55	93.00		
-1.81	223	3.50	127.05		
-1.47	233	4.48	163.25		
-1.11	243	5.55	202.00		
-0.75	253	6.65	242.00		
-0.38	263	7.89	287.00		
0	273	8.11	295.00		
.39	283	8.25	300.00		
.79	293	8.38	305.00		
1.09	300	8.38	305.00